construction materials

MDPI

Review

Flexural and Shear Strengthening of Reinforced-Concrete Beams with Ultra-High-Performance Concrete (UHPC)

Farabi Bin Ahmed [1,†], Rajib Kumar Biswas [2,*,†], Debasish Sen [3] and Sumaiya Tasnim [3]

[1] Department of Civil & Environmental Engineering, South Dakota State University, Brookings, SD 57007, USA; farabibin.ahmed@jacks.sdstate.edu
[2] Okumura Corporation, Tsukuba 300-2641, Japan
[3] Department of Civil Engineering, Ahsanullah University of Science and Technology, 141 & 142, Love Road, Tejgaon Industrial Area, Dhaka 1208, Bangladesh; debasish.ce@aust.edu (D.S.); sumaiyatasnim133@gmail.com (S.T.)
* Correspondence: rajibkumar.biswas@okumuragumi.jp
† These authors contributed equally to this work.

Abstract: Ultra-high-performance concrete (UHPC) is considered to be a promising material for the strengthening of damaged reinforced concrete (RC) members due to its high mechanical strength and low permeability. However, its high material cost, limited code provisions, and scattered material properties limit its wide application. There is a great need to review existing articles and create a database to assist different technical committees for future code provisions on UHPC. This study presents a comprehensive overview focusing on the effect of the UHPC layer on the flexural and shear strengthening of RC beams. From this review, it was evident that (1) different retrofitting configurations have a remarkable effect on the cracking moment compared to the maximum moment in the case of flexural strengthening; (2) the ratios of the shear span and UHPC layer thickness have a notable effect on shear strengthening and the failure mode; and (3) different bonding techniques have insignificant effects on shear strengthening but a positive impact on flexural strengthening. Overall, it can be concluded that three-side strengthening has a higher increment range for flexural (maximum, 81%–120%; cracking, 300%–500%) and shear (maximum, 51%–80%; cracking, 121%–180%) strengthening. From this literature review, an experimental database was established, and different failure modes were identified. Finally, this research highlights current issues with UHPC and recommends some future works.

Keywords: UHPC; flexural and shear failure; RC beam; strengthening

Citation: Ahmed, F.B.; Biswas, R.K.; Sen, D.; Tasnim, S. Flexural and Shear Strengthening of Reinforced-Concrete Beams with Ultra-High-Performance Concrete (UHPC). *Constr. Mater.* **2024**, *4*, 468–492. https://doi.org/10.3390/constrmater4020025

Received: 21 November 2023
Revised: 29 March 2024
Accepted: 21 May 2024
Published: 31 May 2024

1. Introduction

RC structural members are expected to efficiently transfer the loads over the expected service life of the structure. Nevertheless, due to several reasons, which include faults in the design section, changes in building occupancy, deleterious agents that lead to rebar corrosion, low-quality materials, and changes in natural conditions, the structural members may not be expected to last the full life cycle [1–9]. Therefore, strengthening such structural members is often necessary with minimal functional hindrances and at minimum cost [10]. Structures strengthened with normal concrete may demonstrate a decreased resistance within a short period [11]. To resolve this issue, over the past two decades, researchers have developed different approaches for repairing these damaged members. Some of the popular and available methods of retrofitting are external pre-stressing, steel or concrete jacketing, fiber-reinforced polymers, and near-surface mounting [12–28]. Although these techniques are highly effective, certain drawbacks exist. The drawbacks include an increase in dead load in the case of concrete jacketing, the corrosion of steel plates, debonding, long-term durability, fire sensitivity, the inferior performance of carbon fiber reinforced

polymers under cyclic loading and compression, and aging of adhesion materials in the case of fiber reinforced polymers [29–31].

In the past few decades, researchers have investigated the utilization of a new class of cementitious material, ultra-high-performance fiber-reinforced concrete (UHPC), to strengthen damaged RC members [32–42]. UHPC has drawn the attention of researchers mainly for two reasons: superior mechanical properties compared to normal concrete and long durability [43–49]. UHPC exhibits 3 to 5 times higher compressive strength and 2–3 times higher tensile strength than normal concrete. These superior mechanical attributes are observed independently of the different sizes and types of aggregates used in the concrete mix, depending upon the specific range of coarse aggregates utilized in the concrete composition, which closely packs raw materials by different packing models [50,51]. UHPC also offers a dense microstructure with a low water–cement ratio and different pozzolanic materials such as silica fume, thus providing improved resistance against deleterious materials and thermal loads [52–56]. Moreover, UHPC also has the ability to control cracks due to the bridging effect between fiber and surrounding concrete. Therefore, RC structures strengthened with UHPC overlay will greatly improve the serviceability and life cycle of the rehabilitated concrete structures [57–59]. With superior mechanical and durability properties, UHPC has been implemented in a variety of infrastructures to optimize the design of structural elements and extend the service life of infrastructure [60–62].

UHPC has started to gain popularity for structural retrofitting due to its numerous advantages [63]. However, its widespread application is still limited due to higher manufacturing costs compared to traditional concrete [64–68]. Despite the initial construction expenses, it has been observed that the overall life cycle maintenance cost of UHPC (Strategy A) is lower than that of normal concrete (Strategy B), making it a cost-effective choice in the long term (see Figure 1) [11]. Moreover, immature construction technology and lack of design codes are a couple shortcomings that also limit its wide practical application [69]. However, some efforts have been made to establish design standards such as AFGC [70] and JSCE [71] to facilitate the application of UHPC. When some groups of researchers started investigating the impact of parameters like the layer thickness ratio, configurations, position, and bonding methods on retrofitted structures through experimental studies, they found a positive impact [38,72–75]. However, there is a need for a comprehensive literature study to consolidate these findings and understand their effects or challenges such as immature construction technology and lack of design codes hindering its practical application. Therefore, the current study aims to provide an updated overview of research on flexural and shear strengthening of RC beams using UHPC as a repair material. It begins with establishing an experimental database through this literature review, analyzing the effects of different parameters on both flexural and shear strengthening. Various failure modes and the influence of UHPC on these modes are discussed. Finally, current challenges and future research directions in the field of UHPC are addressed.

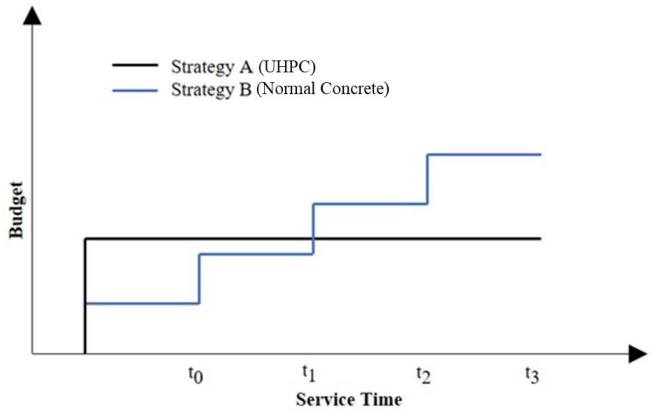

Figure 1. Life cycle cost analyses of two different strengthening materials [11].

2. Effect on Flexural Strength

UHPC is used as an overlay in different configurations to improve the flexural capacity of concrete elements. Several research groups examined the effect of different retrofitting techniques including layer configurations, bonding techniques, and thickness ratios. The experimental outcomes are summarized in Table 1. The experimental outcome of thirty-six beams was included in the experimental database for flexural strengthening of RC beams with UHPC. In the following sections, the effects of different parameters are discussed based on the database presented in Table 1. In order to compare the effectiveness of strengthening by UHPC in the different literature, the cracking and maximum load obtained by experiments were normalized by Equation (1) compared with no strengthened beams or slabs.

$$\text{Flexural strength increment } (\%) = (M - M_{no}/M_{no}) \times 100 \quad (1)$$

where M represents the strengthened moment of UHPC-RC members and M_{no} represents corresponding moments of no strengthened beams or slabs.

Table 1. Summary of flexural strengthening with UHPC layer.

Reference	Sample Name	Beam Dimension, b × h × L (mm)	Loading System	Strengthening Configuration	Reinforcement Ratio, ρ (%)	Steel Fiber Percentage	UHPC Compressive Strength (MPa)	Bonding Method	Thickness, t (mm)	Maximum Load (kN)	Cracking Load (kN)	Failure Modes
Tanarslan et al. [30]	BEAM-1	150 × 250 × 3200	TP [12]	NS [1]	0.905	-	-	-	-	43.21	10.52	CC [3]
	BEAM-2	150 × 250 × 3200	TP	TnS [2]	0.905	3	204	Epoxy	30	48	23.05	CC
	BEAM-3	150 × 250 × 3200	TP	TnS	0.905	3	204	Anchorages	30	52	14.32	RF [4]
Prem and Murthy [32,41]	A	100 × 200 × 1500	TP	NS	0.57	-	-	-	-	56.6	-	CC
	A1	100 × 200 × 1500	TP	TnS	0.57	2	170.29	Epoxy	10	54.97	-	CC
	A2	100 × 200 × 1500	TP	TnS	0.57	2	170.29	Epoxy	15	69.91	-	CC
	A3	100 × 200 × 1500	TP	TnS	0.57	2	170.29	Epoxy	20	76.33	-	CC
	B	100 × 200 × 1500	TP	NS	0.90	-	-	-	-	80.62	-	CC
	B1	100 × 200 × 1500	TP	TnS	0.90	2	170.29	Epoxy	10	79.54	-	CC
	B2	100 × 200 × 1500	TP	TnS	0.90	2	170.29	Epoxy	15	91.4	-	CC
	B3	100 × 200 × 1500	TP	TnS	0.90	2	170.29	Epoxy	20	95.5	-	CC
	C	100 × 200 × 1500	TP	NS	1.30	-	-	-	-	106.17	-	CC
	C1	100 × 200 × 1500	TP	TnS	1.30	2	170.29	Epoxy	10	105.77	-	CC
	C2	100 × 200 × 1500	TP	TnS	1.30	2	170.29	Epoxy	15	118.03	-	CC
	C3	100 × 200 × 1500	TP	TnS	1.30	2	170.29	Epoxy	20	122.23	-	CC
Al-Osta et al. [33]	Normal RC—SB—BOTSJ	140 × 230 × 1600	TP	NS	0.53	-	-	-	-	70	16	CC
	RC—SB—2 SJ	140 × 230 × 1600	TP	TnS	0.53	2	128	Sandblast	30	81	33	NCC [6]
	RC—SB—3 SJ	140 × 230 × 1600	TP	TS [5]	0.53	2	128	Sandblast	30	102	41	NCC or UH-PCC [7]
	RC—EP—BOTSJ	140 × 230 × 1600	TP	ThS	0.53	2	128	Sandblast	30	132	90	UHPCC
	RC—EP—2 SJ	140 × 230 × 1600	TP	TnS	0.53	2	128	Epoxy	30	75	47	NCC
	RC—EP—3 SJ	140 × 230 × 1600	TP	TS	0.53	2	128	Epoxy	30	95	44	NCC or UH-PCC
		140 × 230 × 1600	TP	ThS	0.53	2	128	Epoxy	30	129	95	UHPCC
Paschalis [37,72]	P1	150 × 200 × 2200	TP	NS	0.89	-	-	-	-	55.18	24	CC and FC [8]
	P2	150 × 200 × 2200	TP	NS	0.89	-	-	-	-	53.98	20	CC and FC
	Average	-	TP	-	-	-	-	-	-	54.58	22	-
	U1	150 × 200 × 2200	TP	TnS	0.89	3	126	Concrete Chipping	50	54.6	32	CC and FC
	U2	150 × 200 × 2200	TP	TnS	0.89	3	126	Concrete Chipping	50	56.30	28	CC and FC
	Average	-	TP	-	-	3	126	-	-	55.45	30	-
	3SJ1	150 × 200 × 2200	TP	ThS [11]	0.89	3	126	Concrete Chipping	50	119.2	85	FC
	3SJ2	150 × 200 × 2200	TP	ThS	0.89	3	126	Concrete Chipping	50	112	71	FC
	Average	-	TP	-	-	3	126	-	-	115.6	78	FC
Safdar et al. [76]	Normal	250 × 400 × 3000	TP	NS	0.44	-	-	-	-	118.90	30.00	CC
	BU-20	250 × 400 × 3000	TP	CS [9]	0.44	-	156.3	WJ [10]	20	142.20	35.00	UHPCC
	BL-20	250 × 400 × 3000	TP	TnS	0.44	-	156.3	WJ	20	118.90	70.50	CC
	BU-40	250 × 400 × 3000	TP	CS	0.44	-	156.3	WJ	40	148.20	38.50	RF
	BL-40	250 × 400 × 3000	TP	TnS	0.44	-	156.3	WJ	40	145.30	84.25	RF
	BU-60	250 × 400 × 3000	TP	CS	0.44	-	156.3	WJ	60	137.00	39.70	-
	BL-60	250 × 400 × 3000	TP	TnS	0.44	-	156.3	WJ	60	156.30	88.50	RF
Anusree and Anuragi [77]	CB	150 × 200 × 1500	TP	NS	0.36	-	-	-	-	48.7	29.1	FC
	UTS	150 × 200 × 1500	TP	TnS	0.36	3	-	-	50	51.3	34.2	FC
	UCS	150 × 200 × 1500	TP	CS	0.36	3	-	-	50	68.5	34.5	FC
	UTS3	150 × 200 × 1500	TP	ThS	0.36	3	-	-	50	89.2	47.4	FC
Tanarslan [78]	BEAM-1	150 × 250 × 3200	TP	NS	0.905	-	-	-	-	43.21	10.52	CC
	BEAM-2	150 × 250 × 3200	TP	TnS	0.905	3	204	Epoxy	50	67.97	37.12	CC
	BEAM-3	150 × 250 × 3200	TP	TnS	0.905	3	204	Anchorages	50	57.23	19.27	RF

[1] No Strengthening; [2] Tension Side; [3] Concrete Crushing; [4] Rebar Failure; [5] Two Sides; [6] Normal Concrete Crushing; [7] UHPC Crushing; [8] Flexural Crack; [9] Compression Side; [10] Water Jetting; [11] Three Sides; [12] Two Points.

2.1. Effect of UHPC Layer Position

From the existing literature, it can be noted that generally four types of strengthening configurations were considered in the RC beam to examine the effect of flexural strengthening (see Figure 2) [79]. Layer positions are denoted as the compression side, tension side, two sides, and three sides.

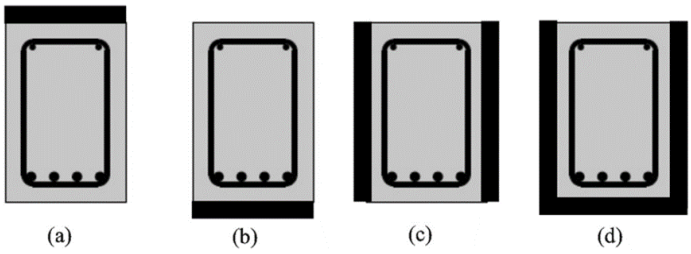

Figure 2. Different configurations of flexural strengthening: (**a**) compression side; (**b**) tension side; (**c**) two sides; and (**d**) three sides. Reprinted with permission from Ref. [79]. Copyright 2020 Elsevier.

Al-Osta et al. [33] applied several bonding techniques (using sandblast and epoxy) and configurations (tension, two, and three sides) for strengthening concrete beams by UHPC. They reported that the beams strengthened with three-side configurations resulted in the highest moment capacity, while beams strengthened only on the tension side demonstrated the least enhancement (Table 1). In another study, Safdar et al. [76] tested an RC beam retrofitted with the UHPC layer at the tension and compression side. This study reported that the cracking load was nearly double in the RC beam retrofitted with UHPC at the tension side than that of the compression side as shown in Table 1.

The experimental findings were analyzed to understand trends in the maximum moment and cracking moment increment across different layer configurations, depicted in Figures 3 and 4. These figures delineate regions denoted as LI, MI, and HI, representing low, medium, and high moment increments, respectively. Notably, configurations featuring three-sided strengthening consistently fell within the HI category in both figures. Moreover, the findings revealed that after flexural strengthening, the increase in the cracking moment is substantially higher than the increase in the maximum moment. This behavior can be attributed to the steel fibers present in UHPC, which leads to a delay in crack opening. Conversely, the maximum moment increment is attributed to several factors: (1) the UHPC layer added on the tension and compression sides, which increased the arms of coupling between the tensile and compression forces, thereby enhancing the flexural capacity (see Figure 5); (2) the UHPC layer added on two sides resulted in an increased beam width; and (3) in the case of the UHPC layer added on three sides, both beam width and couple arms were enhanced (see Figure 5).

To obtain a clear idea of the effectiveness of strengthening RC beams with different configurations of UHPC layers, cracking and maximum moments were normalized with the respective moments obtained for the RC beam strengthened at the tension side. The obtained results are presented in Figure 6. It can be seen that RC beams strengthened at the compression side demonstrated a moment ratio lower than 0.5, whereas other configurations resulted in a moment ratio of more than 1. Thus, it becomes evident that RC beams strengthened at the compression side are less effective compared to other configurations. On the other hand, specimens retrofitted with two and three sides offered a moment ratio higher than 1. This is because, under the neutral axis, the portion of UHPC also resists the tensile load simultaneously with the reinforcement.

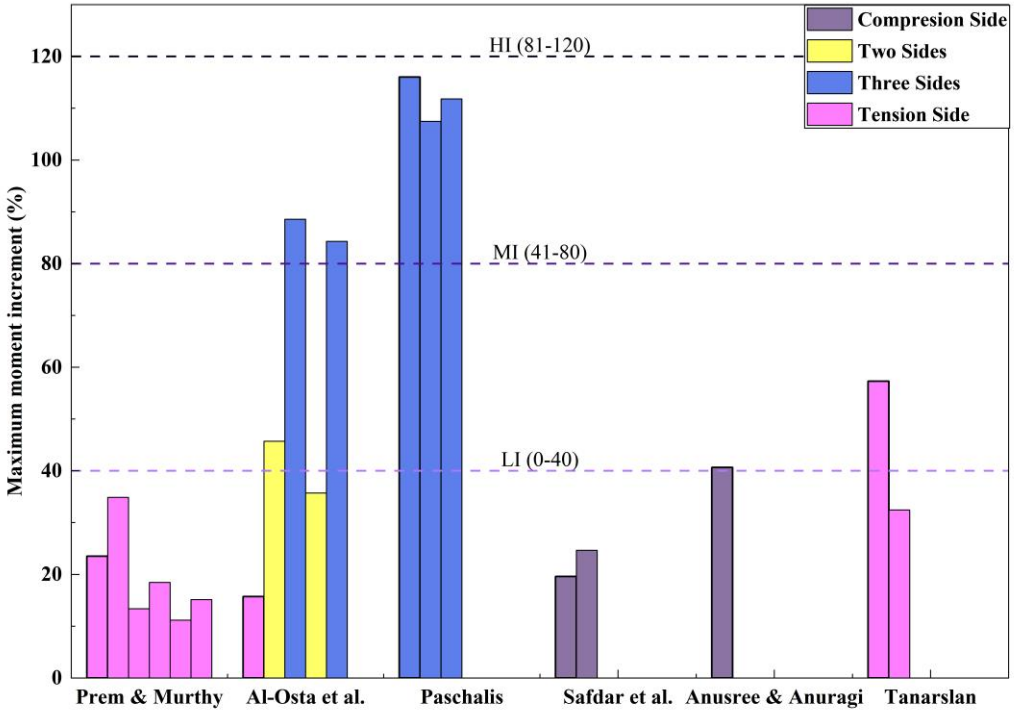

Figure 3. Different configurations of flexural strengthening: (a) compression side; (b) tension side; (c) two sides; and (d) three sides [32,33,41,72,76–78].

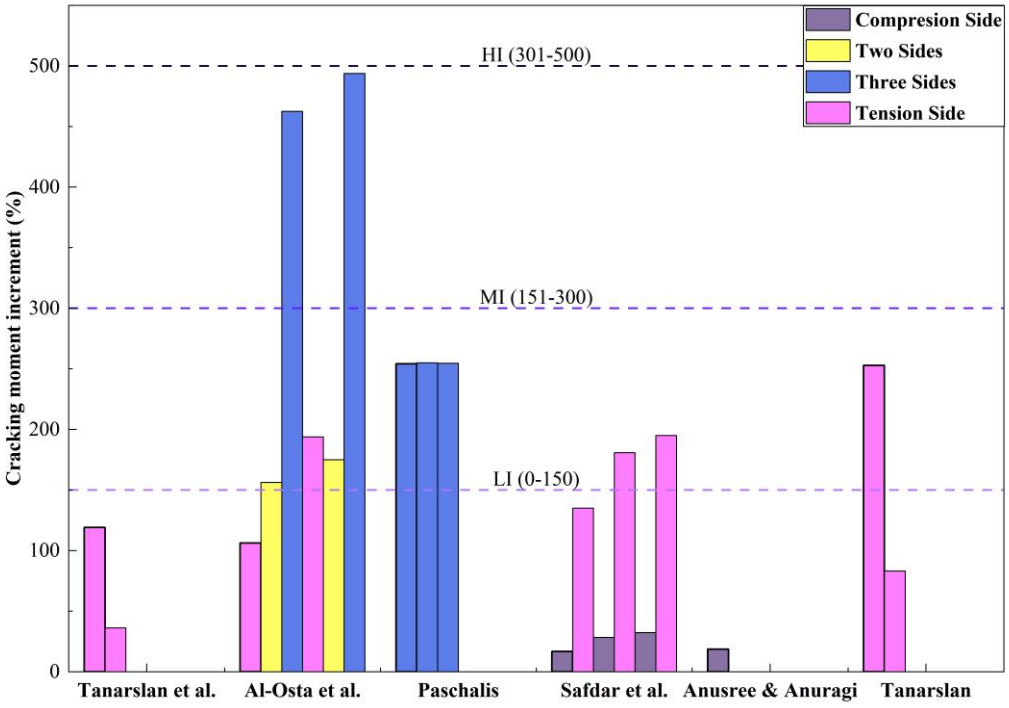

Figure 4. Effect of different configurations of flexural strengthened beams on cracking moment increment [30,33,72,76–78].

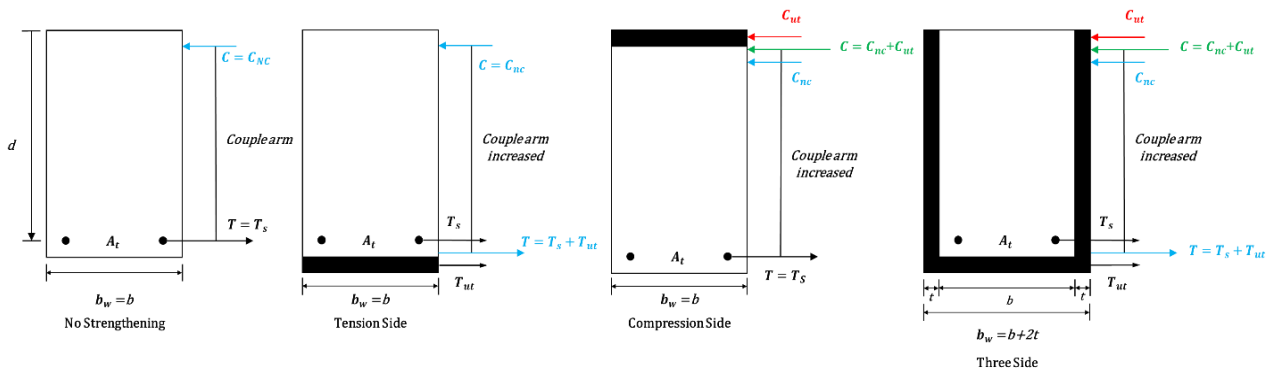

Figure 5. The reasons for the enhancement in moment increment in schematic view.

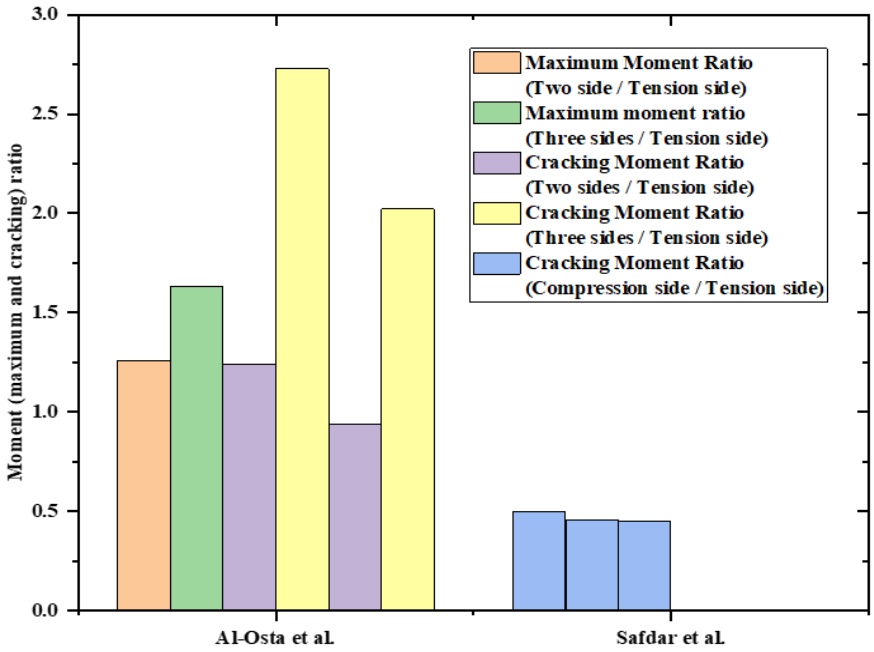

Figure 6. Effect of different strengthening configurations on moment ratio [33,76].

2.2. Effect of Beam Depth and UHPC Layer Thickness Ratio

From the previous experimental studies, it became evident that the ratio of beam depth and UHPC layer thickness (from 5 up to 20) notably affected the moment capacity (Table 1). According to the previous research, it was observed that the percentage of the moment increment (cracking and maximum) was reduced by the increment of beam depth and strengthening thickness ratio (Figures 7 and 8). This means that increasing the UHPC layer thickness enhances the moment capacity. The reasons for the enhancement in the maximum moment increment are as follows: (1) the increment of UHPC layer thickness on tension and compression sides increased the couple arms between the tensile and compression force, resulting in a more enhanced flexural capacity (Figure 5); (2) the increased UHPC layer thickness on two sides, strengthening configuration, resulted in increased beam width; and (3) the increased UHPC layer thickness on three sides, strengthening configuration, enhanced both the beam width and couple arms (Figure 5).

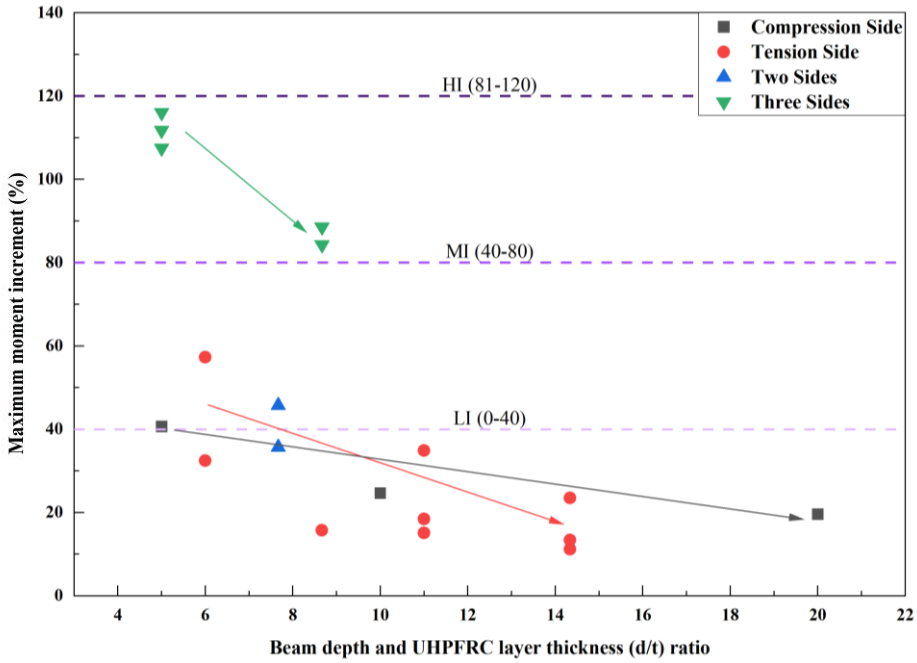

Figure 7. Maximum moment and beam depth and strengthening thickness ratio relation on different configurations of flexural strengthening beams.

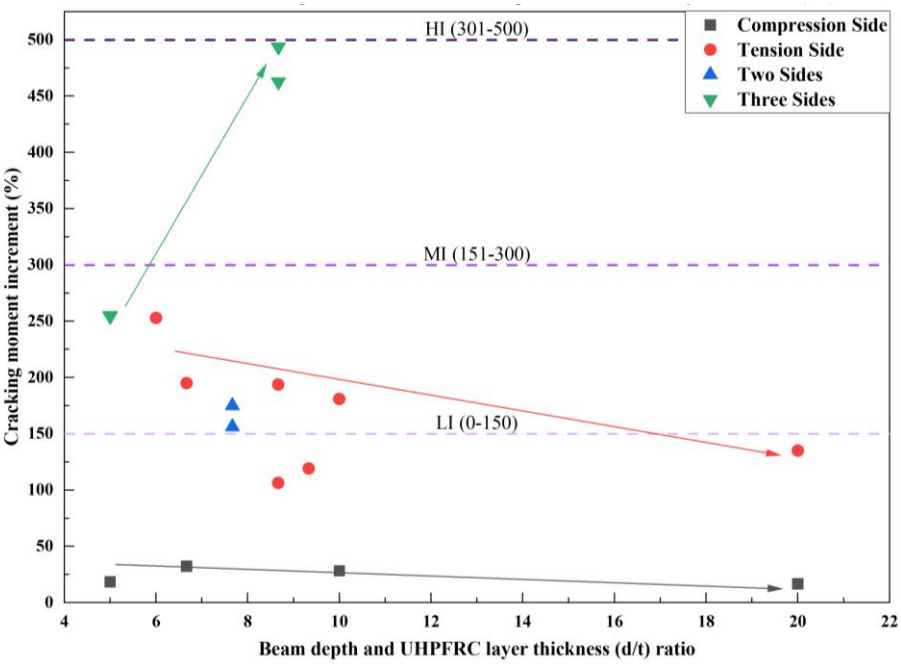

Figure 8. Cracking moment and beam depth and strengthening thickness ratio relation on different configurations of flexural strengthening beams.

The three sides strengthening configurations outperform the other three strengthening configurations in terms of their impact on moment increases (maximum and cracking) as shown in Figures 7 and 8. It is also noted that the tensile side strengthening substantially increases the cracking moment compared to the compression side strengthening; nevertheless, there was no notable difference in the case of the maximum moment as can be seen in Figures 7 and 8. This may occur due to the contribution of fiber that greatly influenced the crack resistance. However, in the case of a maximum moment increment, the effect of fiber can be negligible as fibers might be yielded or ruptured.

Some studies reported that beam depth and UHPC layer thickness ratio decreases did not influence or negatively influence the moment increment. For example, Safdar et al. [76] tested the moment capacity of the RC beam strengthened with UHPC layers with different thicknesses (Figure 9). From the obtained results, it can be seen that a decreased ratio of beam depth and strengthening thickness significantly reduces the maximum moment capacity. This behavior can be attributed to (1) localized macro-cracks between the old concrete structure and the UHPC layer that influence the deterioration of bonds; and (2) the uneven distribution of steel fiber during the UHPC layer preparation. Prem and Murthy [32,41] examined the effect of the UHPC layer on partially damaged beams by applying preload (90% load applied) before retrofitting those beams on the tension side. They noticed that a larger layer thickness is required to see the effect of strengthening in damaged beams (A1, B1, C1).

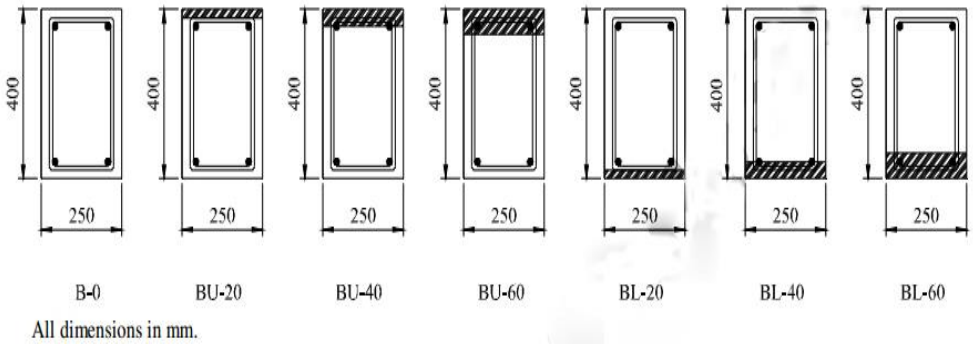

Figure 9. Geometrical view of flexural retrofitted beams with different thicknesses of UHPC layers. Reprinted with permission from Ref. [76]. Copyright 2016 Elsevier.

2.3. Effect of Bonding Techniques

A UHPC layer is attached to different zones of concrete elements to improve flexural capacity. Several research groups examined the effect of different retrofitting techniques, i.e., (a) water jetting; (b) epoxy; (c) the sandblasting method; (d) anchoring; and (e) concrete chipping [72], to strengthen RC beams with UHPC (Figure 10) [33,76,78]. In this section, some key findings are discussed.

Safder et al. [76] emphasized that strength capacity depends on strengthening configurations rather than bonding techniques. On the other hand, several researchers reported that epoxy substantially enhances flexural capacity [32,33,41,78]. For example, Tanarslan [78] reported that epoxy bonding technique beams sustained a higher load to crack than that of the mechanical anchoring bonding technique. In another study, Al-Osta et al. [31] examined the behavior of composite beams bonded with epoxy and sandblast, which concluded that both techniques demonstrate similar performance.

Effective bonding techniques smoothly transfer the load from weak concrete elements to the strengthening portion of the structure and act combinedly as a single structural element. Figure 11 summarizes the influence of different configurations and bonding techniques on the maximum moment. It is noticed that the three-side strengthening configuration with the concrete chipping technique demonstrates the highest maximum moment increment (falls in the high increment range) and the compression side strengthening configuration (falls in the low increment range) with the water jetting technique has the least effect. Figure 12 summarizes the influence of different configurations and bonding techniques on the cracking moment increment. It is found that the highest cracking moment increment is observed in the three-side strengthening configuration (falls in the high increment range) beam with the epoxy bonding technique and the lowest cracking moment increment is observed in the compression side strengthening configuration (falls in the low increment range) with water jetting. In addition, from Figures 11 and 12, it is noteworthy that each bonding technique contributed more to the cracking moment than the maximum moment.

Figure 10. Different bonding techniques of flexural strengthened beams: (**a**) Water jetting. Reprinted with permission from Ref. [76]. Copyright 2016 Elsevier. (**b**) Epoxy. Reprinted with permission from Ref. [33]. Copyright 2017 Elsevier. (**c**) Sandblasting method. Reprinted with permission from Ref. [33]. Copyright 2017 Elsevier. (**d**) Anchoring. Reprinted with permission from Ref. [30]. Copyright 2017 Elsevier. (**e**) Concrete chipping. Reprinted with permission from Ref. [72]. Copyright 2017 Elsevier.

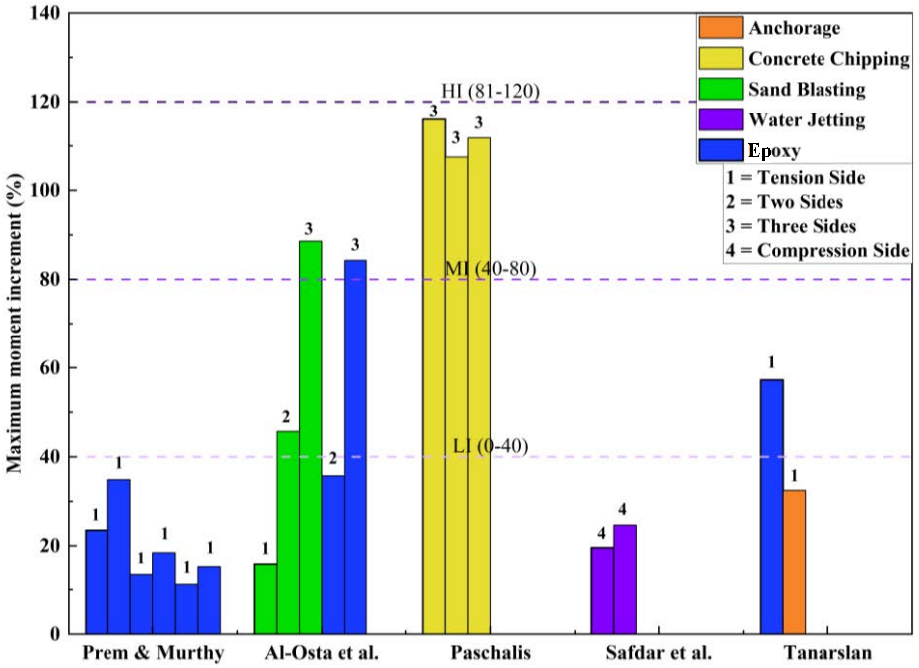

Figure 11. Different bonding techniques of flexural strengthening beam effects on % of maximum moment increment [32,33,41,72,76,78].

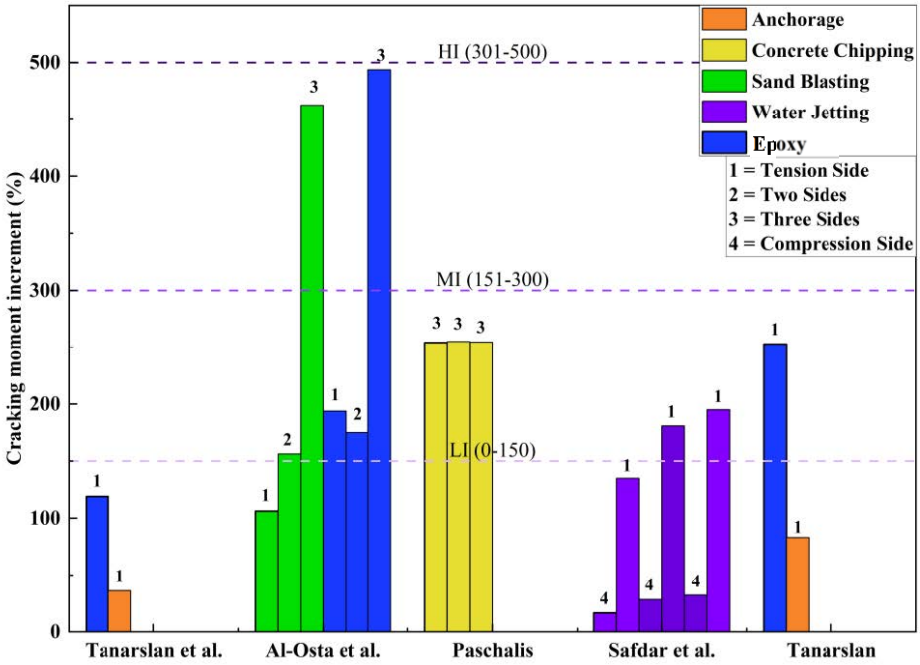

Figure 12. Different bonding techniques of flexural strengthening beam effects on % of cracking load increment [30,33,72,76,78].

2.4. Effect of Compressive Strength

It can be seen from the available experimental results that the maximum moment is generally enhanced as compressive strength increases (Figure 13). This means that the compressive strength increment moderately enhances the maximum moment capacity. However, for three-side strengthening, the percentage of the maximum moment increment decreases due to the debonding of the UHPC layer after a crack, causing it to act separately. Figure 14 shows a significant amount of improvement in the crack moment increments for all types of strengthening.

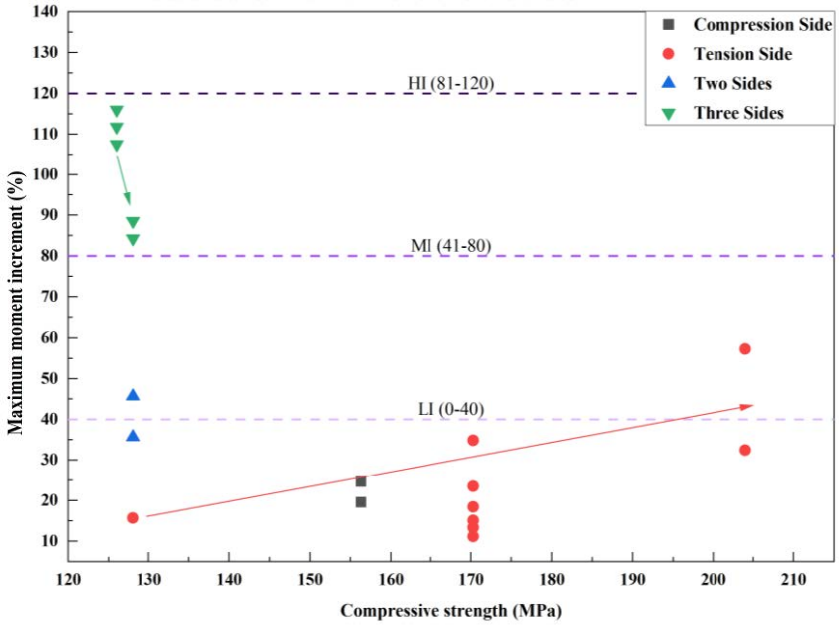

Figure 13. Effect of compressive strength on maximum moment.

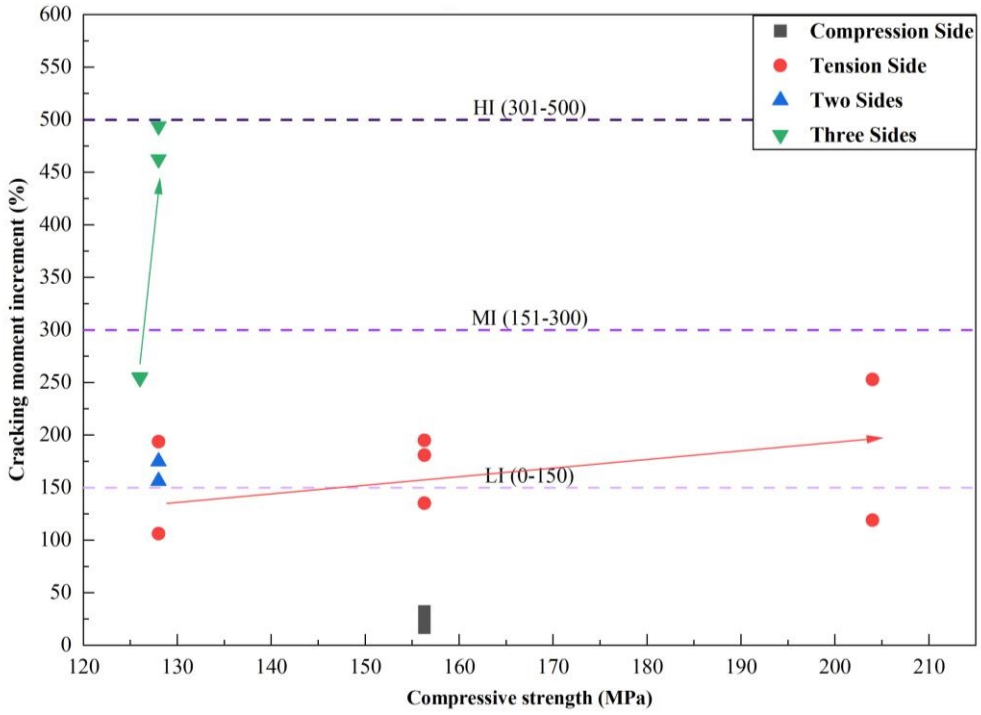

Figure 14. Effect of compressive strength on cracking moment.

2.5. Effect of Steel Fiber Percentage

From the existing literature, it can be noted that generally two to three percent of steel fiber was used in UHPC. From all the summarized studies, it appears that the percentage of the moment increment (cracking and maximum) increases as the steel fiber percentage increases (Figures 15 and 16). This means that the steel fiber percentage increment enhances the moment capacity. It is further observed that the increase in the cracking moment is substantially larger than that of the maximum moment (Figures 15 and 16). This behavior can be attributed to the steel fiber presence in UHPC, which leads to delayed crack opening.

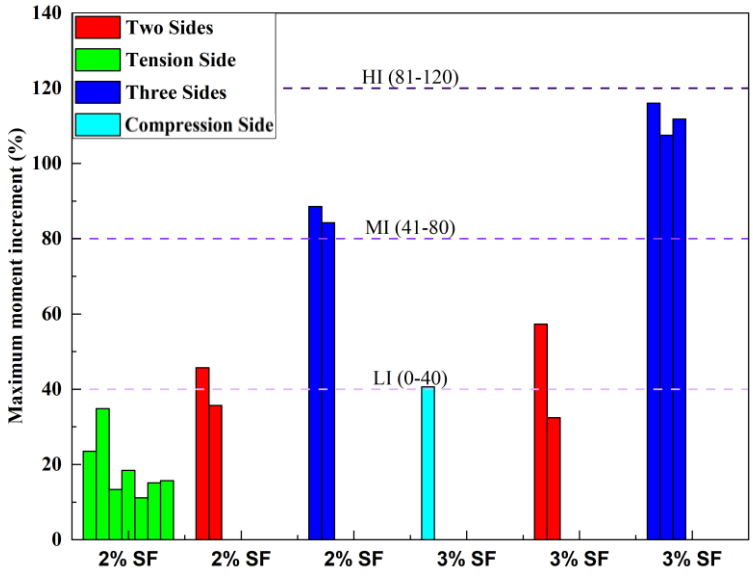

Figure 15. Effect of steel fiber percentage on maximum moment.

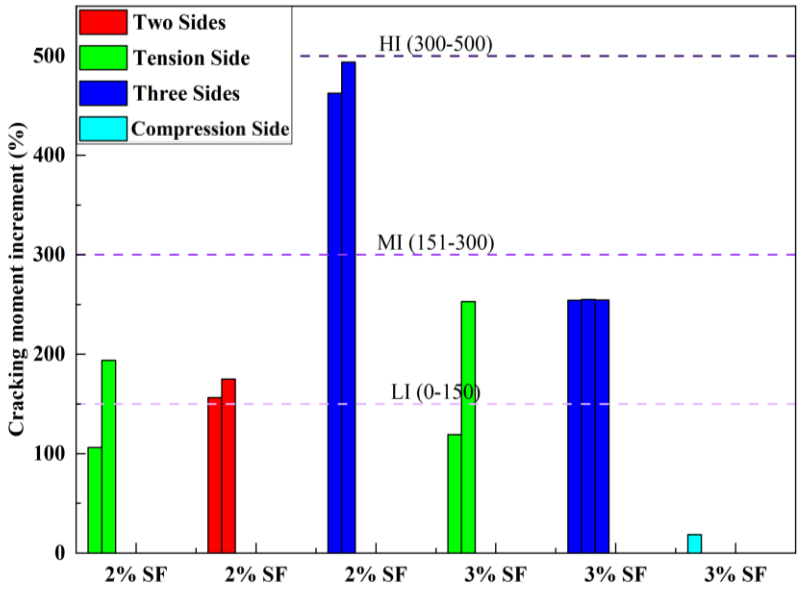

Figure 16. Effect of steel fiber percentage on cracking moment.

3. Effect on Shear Strength

Traditionally, a reinforced concrete jacket is applied to increase the cross-section area of RC beams to improve the shear resistance; however, it adds additional self-weight [80]. In order to minimize the self-weight enhancement, researchers endeavored to achieve shear improvement by the application of the UHPC jacket, which can be an effective strengthening method. A significant number of past studies have been investigated to understand the effect of UHPC strengthening, with varying configurations, and various bonding, UHPC compressive strengths, and steel–fiber ratios. The outcomes from past studies are provided in Table 2. All of these previous studies illustrated that before strengthening, those beams failed due to shear deficiency. However, after UHPC strengthening, it demonstrated a notable impact on load-carrying capacity and the failure mode. In order to compare the effectiveness of strengthening by UHPC in the different literature, the cracking and

maximum load obtained by experiments were normalized by Equation (2) compared with no strengthened beams or slabs.

$$\text{Shear strength increment } (\%) = (V - V_{no} / V_{no}) \times 100 \quad (2)$$

where V represents the strengthened shear force of UHPC-RC members and V_{no} represents the corresponding shear force of no strengthened beams or slabs.

Table 2. Summary of shear strengthening with UHPC layer.

Reference	Sample Name	Beam Dimension, b × h × L (mm)	Loading System	Steel Fiber Percentage	UHPC Compressive Strength (MPa)	Strengthening Configuration	Bonding Method	Thickness, t (mm)	Shear Span, a (mm)	Maximum Load (kN)	Cracking Load (kN)	Failure Modes
Bahraq et al. [73,74]	CT-1.0	140 × 230 × 1120	TP [10]	-	-	NS [1]	-	-	600	383	-	S [4]
	SB-2SJ-1.0	140 × 230 × 1120	TP	2	151.4	TS [2]	Sandblast	30	600	567	-	F-S [5]
	SB-3SJ-1.0	140 × 230 × 1120	TP	2	151.4	ThS [3]	Sandblast	30	600	628	-	F [6]
	EP-2SJ-1.0	140 × 230 × 1120	TP	2	151.4	TS	Epoxy	30	600	529	-	F–S
	EP-3SJ-1.0	140 × 230 × 1120	TP	2	151.4	ThS	Epoxy	30	200	625	-	F–S
	CT-1.5	140 × 230 × 1120	TP	-	-	NS	-	-	200	286	-	S
	SB-2SJ-1.5	140 × 230 × 1120	TP	2	151.4	TS	Sandblast	30	200	402	-	F–S
	SB-3SJ-1.5	140 × 230 × 1120	TP	2	151.4	ThS	Sandblast	30	200	482	-	F
	EP-2SJ-1.5	140 × 230 × 1120	TP	2	151.4	TS	Epoxy	30	200	435	-	F–S
	EP-3SJ-1.5	140 × 230 × 1120	TP	2	151.4	ThS	Epoxy	30	280	487	-	F
	CT-2.0	140 × 230 × 1120	TP	-	-	NS	-	-	384	276	-	S
	SB-2SJ-2.0	140 × 230 × 1120	TP	2	151.4	TS	Sandblast	30	384	346	-	F–S
	SB-3SJ-2.0	140 × 230 × 1120	TP	2	151.4	ThS	Sandblast	30	384	353	-	F
Hor et al. [75]	RE-0	300 × 100 × 1600	OP [11]	-	-	NS	-	-	600	61.08	-	S
	RE-20	300 × 100 × 1600	OP	3	153	TnS	CC	20	600	57.18	-	F–S
	OV-25	300 × 100 × 1600	OP	3	153	TnS [7]	CC [8]	25	600	73.47	-	S
	OV-50	300 × 100 × 1600	OP	3	153	TnS	CC	50	600	77.97	-	S
Sakr et al. [81,82]	C-S	150 × 300 × 2000	TP	-	-	NS	-	-	525	115	48	S
	ST-2S	150 × 300 × 2000	TP	2	135.37	TS	Epoxy	30	525	281	93	F
	ST-1S	150 × 300 × 2000	TP	2	135.37	OS [9]	Epoxy	60	525	153	60	F-S
Aghani and Afshin [83]	S1	100 × 200 × 1500	OP	-	-	NS	-	-	650	58.1	-	S
	S2	100 × 200 × 1500	OP	-	-	NS	-	-	650	59.7	-	S
	S3-re	100 × 200 × 1500	OP	2	140	TS	Epoxy	30	650	73	-	F
	S4-re	100 × 200 × 1500	OP	2	140	TS	Epoxy	30	650	72.3	-	F
Tanarslan et al. [84]	BEAM-1	150 ×250 × 3200	TP	-	-	NS	-	-	1000	84.74	18.12	S
	BEAM-2	150 ×250 × 3200	TP	2.75	-	TS	Epoxy	30	1000	118.81	21.05	S
	BEAM-3	150 ×250 × 3200	TP	2.75	-	TS	Anchorage	30	1000	107.18	29.47	S
	BEAM-4	150 ×250 × 3200	TP	2.75	-	TS	Epoxy	50	1000	124.85	23.53	F
	BEAM-5	150 ×250 × 3200	TP	2.75	-	TS	Anchorage	50	1000	125.02	25.27	F
	BEAM-6	150 ×250 × 3200	TP	2.75	-	TS	Epoxy	30	1000	124.79	21.55	F
He and Chao [85,86]	RC-2.7	200 × 500 × 2700	OP	-	-	NS	-	-	1350	655	-	S
	RC-U-2.7	200 × 500 × 2700	OP	2.5	150	TnS	CC	50	1350	717	-	S
Wirojjanapirom et al. [87,88]	Ref	250 × 300 × 1800	TP	-	-	NS	-	-	720	138	-	-
	UFC20-S	250 × 300 × 1800	TP	2	194.7	ThS	CC	20	720	319.6	-	S
	UFC20-SB	250 × 300 × 1800	TP	2	192.6	ThS	Anchorage	20	720	355.8	-	S
Asmaa et al. [89]	B0	120 × 250 × 1700	TP	-	-	NS	-	-	500	133.72	38.151	S
	B1	120 × 250 × 1700	TP	1.5	113.73	TS	CC	25	500	141.26	79.556	S
	B2	120 × 250 × 1700	TP	1.5	113.73	TS	CC	35	500	156.95	91.946	S
	B3	120 × 250 × 1700	TP	3	121.1	TS	CC	25	500	187.37	95.617	F
	B4	120 × 250 × 1700	TP	3	121.1	TS	CC	35	500	186.89	91.154	F
	B5	120 × 250 × 1700	TP	3	121.1	OS	CC	25	500	150.31	88.79	S
	B6	120 × 250 × 1700	TP	3	121.1	ThS	CC	35	500	199.73	99.721	F
	B7	120 × 250 × 1700	TP	3	121.1	TS	CC	25	500	166.9	86.722	F
	B8	120 × 250 × 1700	TP	3	121.1	TS	Anchorage	25	500	154.18	80.359	F
	B9	120 × 250 × 1700	TP	3	121.1	TS	Anchorage	25	500	148.66	75.618	F–S
	B10	120 × 250 × 1700	TP	3	121.1	TS	Anchorage	25	500	147.55	73.549	F
	B11	120 × 250 × 1700	TP	3	121.1	TS	Anchorage	25	500	150.13	80.312	F
Nadir et al. [90]	B	150 × 250 × 1500	TP	2	-	-	-	-	600	109.8	-	S
	B30	150 × 250 × 1500	TP	2	133.8	TS	Epoxy	30	600	228.3	-	F
	B30S	150 × 250 × 1500	TP	2	133.8	TS	Epoxy	30	600	207.5	-	F–S

[1] No Strengthening; [2] Two Sides; [3] Three Sides; [4] Shear; [5] Flexure–Shear; [6] Flexure; [7] Tension Side; [8] Concrete Chipping; [9] One Side; [10] Two Points; [11] One Point.

3.1. Effect of UHPC Layer Position

Generally, four types of strengthening configurations (denoted as one side, tension side, two sides, and three sides as shown in Figure 17) were considered in the literature to strengthen the RC beam. In recent years, some researchers have used the UHPC

layer for strengthening purposes, keeping shear improvement in mind [73,74]. Most of the researchers used two-side and three-side retrofitting configurations, whereas few researchers used tension-side and one-side strengthening configurations, as shown in Figure 17a–d. Considering different strengthening configurations (two sides and three sides) and bonding techniques (sandblast and epoxy), Bahraq et al. [73,74] demonstrated that the UHPC strengthening improved the maximum load significantly when compared to un-strengthened specimens. The experimental observation showed that the percentage of maximum load reduction mainly depends on the shear-span-to-effective-depth ratio (a/d) as well as failure modes (Table 2).

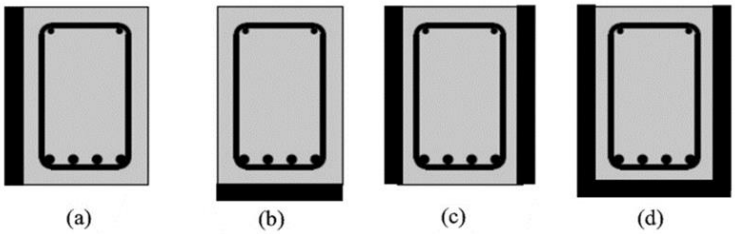

Figure 17. Different configurations of shear strengthening beams: (**a**) one side; (**b**) tension side; (**c**) two sides; and (**d**) three sides.

In order to understand the effect of layer position, the improvements in maximum and cracking load capacity with different layer configurations are plotted in Figures 18 and 19, respectively. The results show that the three-side strengthening can give higher ultimate load capacity improvement (falls in the high increment range) when compared to other configurations, whereas the tension-side strengthening can give a lower extent of ultimate capacity improvement (falls in the low increment range). Meanwhile, the cracking load capacity increment improvement for three-side strengthening (falls in the high increment range) varies between ~85% and 160%. On the other hand, the cracking load capacity enhancement for two-side and one-side strengthening varies between ~15% and 145% and ~25% and 130%, respectively. The dispersion of the percentage of cracking capacity improvement can be attributed to the variation in the bonding technique. It also changes the cracking pattern of the RC beam from the shear to the flexural along with a larger deflection capacity (Figure 20). In the case of two two-side or three-side strengthening configurations, the UHPC layer acted as vertical reinforcement that shifted the failure mode from pure shear to flexure–shear or the flexural mode [83].

Previous experimental studies depicted that the different strengthening configurations affect the failure modes. It was observed by the researchers that a three-side strengthening beam changed the failure mode from shear failure to flexural failure in most of the cases [73,74]. This behavior was expected for the following reasons: (1) The effective depth is increased. Therefore, the a/d ratio will be decreased, resulting in a more enhanced shear capacity of the section compared to flexural capacity. (2) There is a comparatively higher shear strength gain in two sides that pushes the longitudinal steel that starts to yield prior to the shear failure. However, when considering a two-side strengthening beam, mainly two types of failure modes were noticed including (1) flexure–shear [73,74]; (2) flexural [81–84]. The beam failed in the combined flexure–shear or flexural mode because UHPC strips acted as vertical reinforcement to carry more shear load in addition to the contribution of the shear stirrups and the concrete toward the total shear capacity. This enhanced shear capacity of the beam resulted in an increase in the failure load and a shifting of the failure mode from pure shear to flexure–shear or the flexural mode.

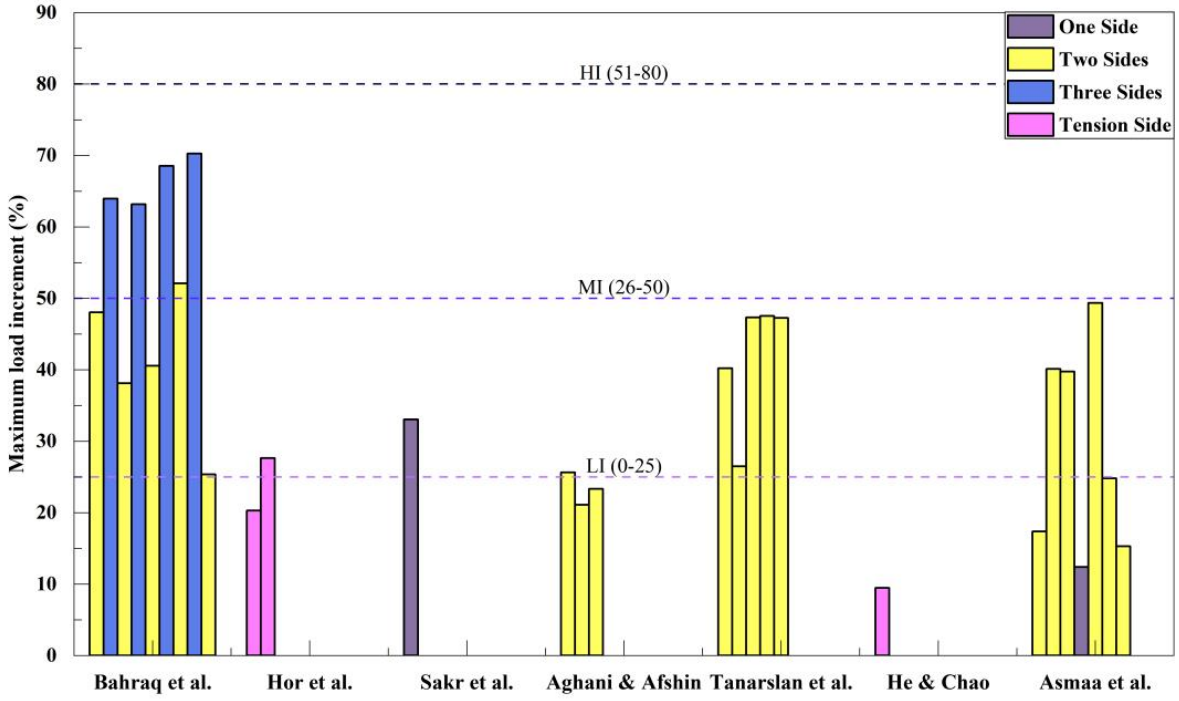

Figure 18. Effects of different configurations on maximum load [73–75,81–86,89].

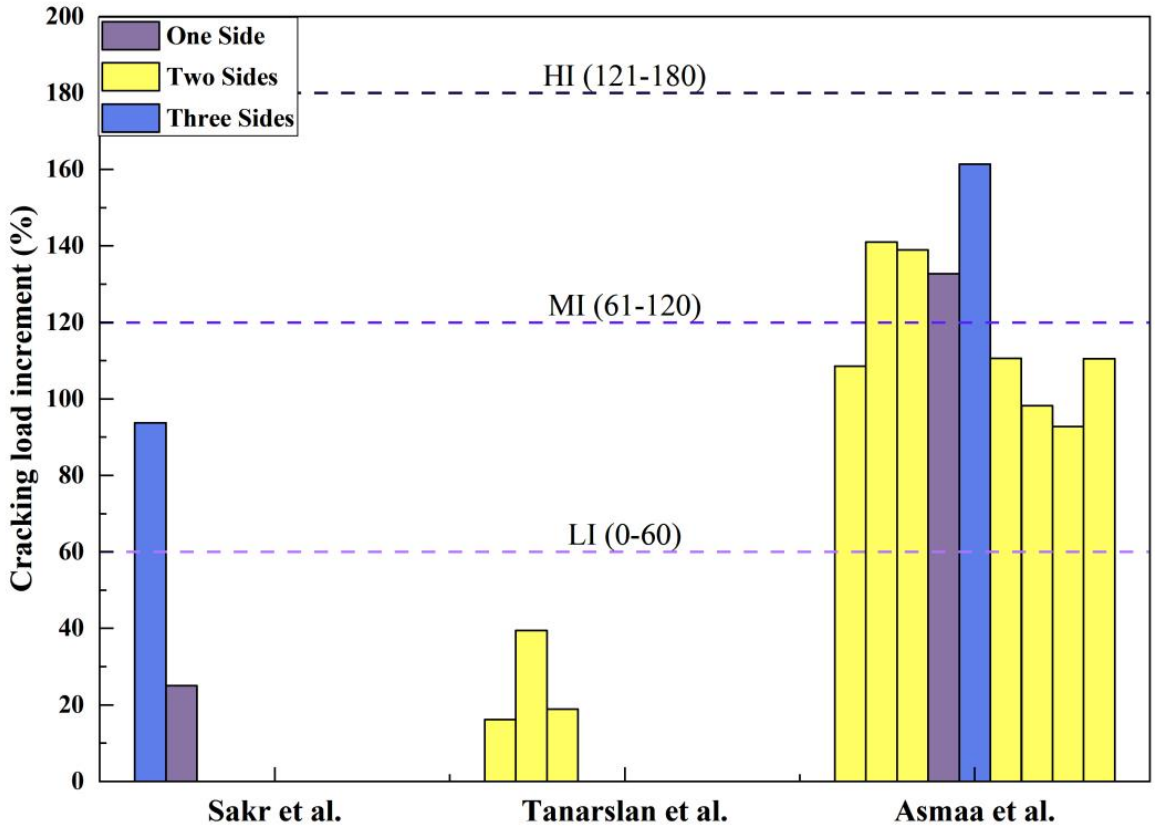

Figure 19. Effects of different configurations on cracking load [81,82,84,89].

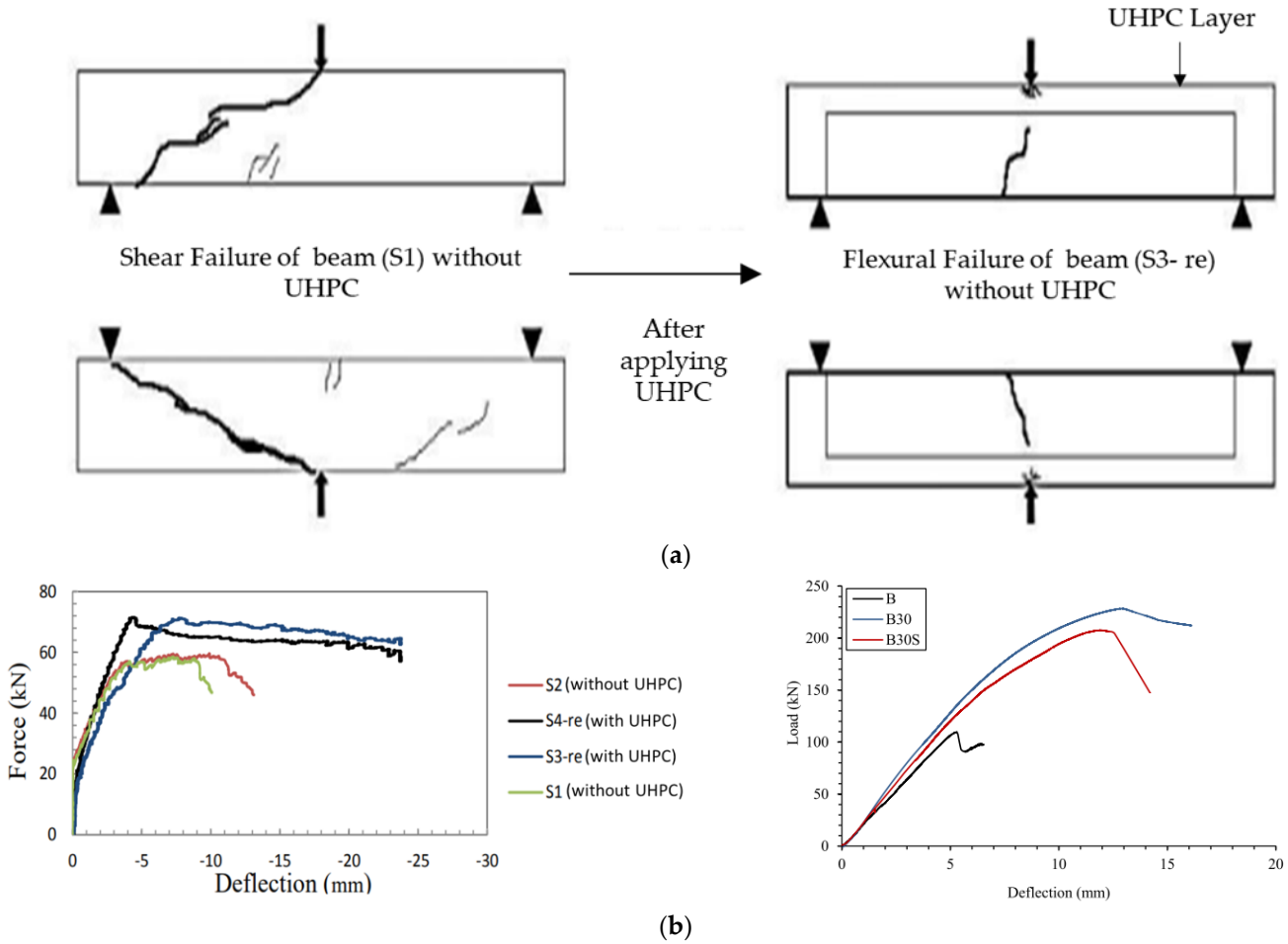

Figure 20. Effect of UHPC layers on shear-strengthened beams: (**a**) in cracking patterns, adapted from Ref. [83], and (**b**) in deformations (force vs. deflection), reprinted from Ref. [83], and others (load vs. deflection), reprinted with permission from Ref. [90]. Copyright 2023 Elsevier.

3.2. Effect of Shear Span and UHPC Layer Thickness Ratio

From the results of various experiments, it is evident that the shear span and strengthening thickness ratio (0 up to 35) notably affected the load-carrying capacity (Table 2) but have not been in agreement. For example, Hor et al. [75] showed that load capacity enhancement decreased with the increase in the shear span and strengthening thickness ratio in the case of a tension-side-strengthened slab. Alternatively, Bahraq et al. [73,74] tested the shear strength of the beam by different configurations (two- and three-side strengthening) of the UHPC layer attachment and it was found that the load capacity improved until a certain ratio of the shear span and strengthening thickness. After that point, the load-carrying capacity improvement fell down, although the shear span and strengthening thickness ratio increased, as shown in Table 2.

Despite all of this prior research being summarized, it appears that when the shear span and strengthening thickness ratio increased, the percentage of the maximum load increment nonlinearly decreased for various strengthening configurations (Figure 21). The reasons for the reduction in the percentage of the maximum load increment are (1) a constant UHPC thickness with a higher shear span reduces the load-carrying capacity by reducing the effectiveness of the arch action and dowel action; (2) a constant shear span with a lower UHPC thickness reduces the load-carrying capacity by reducing the total concrete area. However, in the case of the cracking moment as the shear span and strengthening thickness ratio increases, the percentage of the cracking moment increment also goes down.

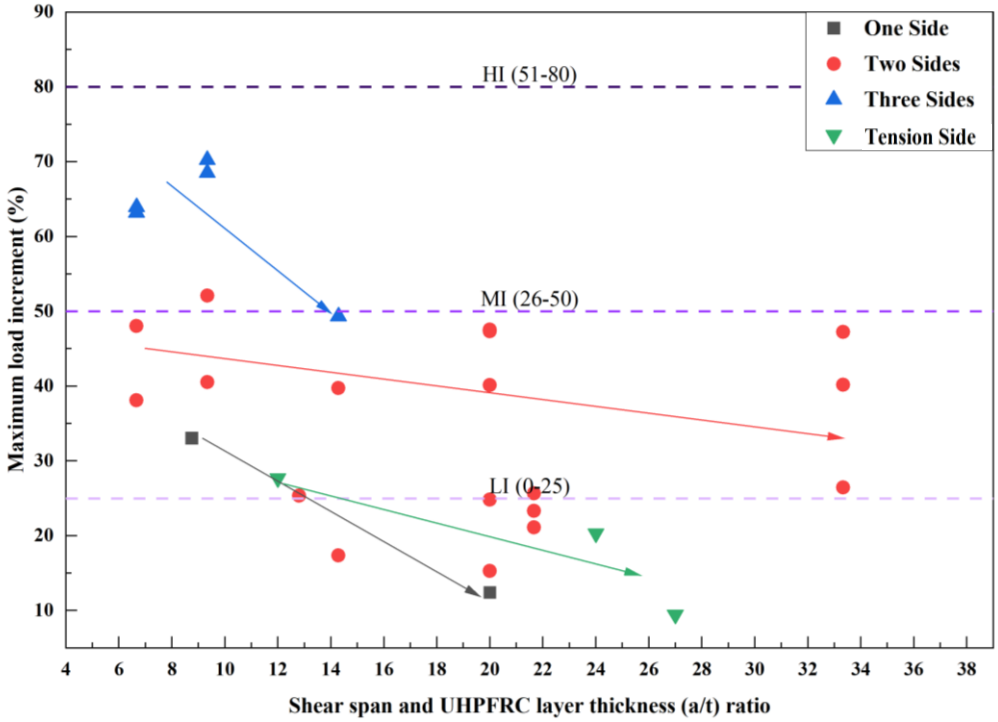

Figure 21. Relation between maximum load and shear span and UHPC layer thickness (a/t) ratio [73–75,81–84,89].

Several researchers highlighted that the failure mode was affected by the increment of the shear span and strengthening thickness ratio. For example, Tanarslan et al. [84] reported that the rising in the shear span and strengthening thickness ratio in the two-side strengthening configuration completely changes the failure mode of a beam from flexural failure (BEAM-4) to shear failure (BEAM-2). It means that the reduction in the UHPC layer reduces the concrete shear capacity area. This reduces the shear capacity of the beam, resulting in a decrease in the failure load and a shifting of the failure mode from flexural failure to shear.

3.3. Effect of Bonding Techniques

The most common bonding techniques of beam strengthening that have been observed in previous studies are (a) concrete chipping; (b) gluing with epoxy; (c) the sandblasting method; and (d) mechanical anchoring (Figure 10). The improvements in maximum and cracking load capacity with different bonding techniques are plotted in Figures 22 and 23, respectively, to understand the effect of bonding techniques. It becomes evident, from Figure 22, that maximum load improvement for a particular strengthening configuration (i.e., one side, tension side, two sides, and three sides) depends to a lesser extent on bonding techniques (Figure 23) as long as the connected surface strength is enough to resist the debonding; rather, the analysis result advocates for the influence of strengthening configurations on the improvement in load-carrying capacity of the beam. Figure 22 summarizes the influence of different strengthening configurations and bonding techniques on the improvement in the maximum load-carrying capacity of the beam. Meanwhile, the cracking load capacity improvement varies between ~20% and 140% for two-side strengthening with the variation of bond techniques (Figure 23). From the studied experimental results, it becomes evident that concrete chipping and anchorage, during two-side strengthening, performed better to improve the cracking capacity of the RC beam.

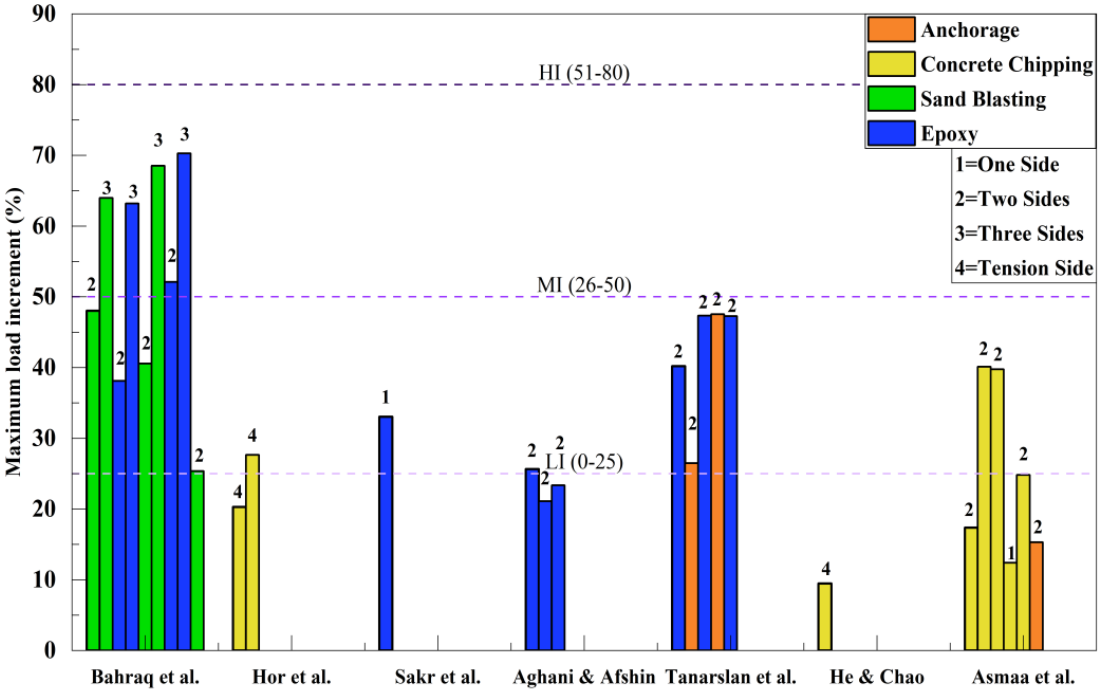

Figure 22. Different bonding techniques' effect on maximum load increment [73–75,81–86,89].

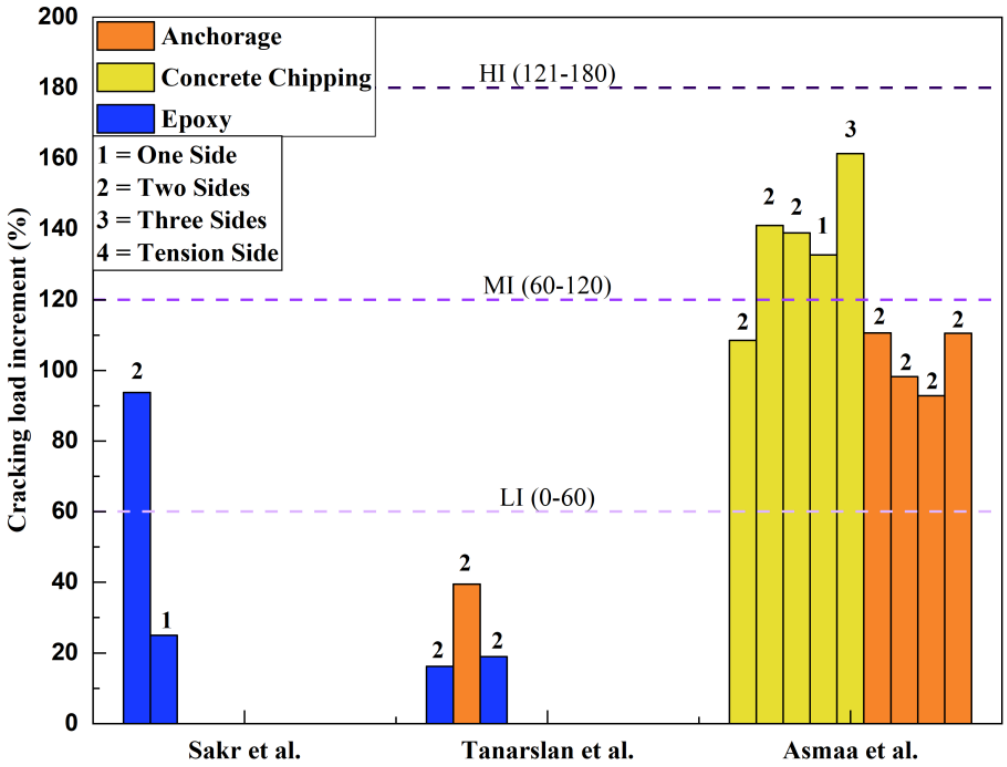

Figure 23. Different bonding techniques' effect on cracking load increment [81,82,84,89].

In addition, the complications of bonding techniques of UHPC regarding a strengthened RC beam are investigated. Bahraq et al. [73,74] reported a specific complication about three-sided jacketing with an epoxy adhesive. The problem was a mismatching between the bottom-retrofitted layer and the two-side strengthening layers. After cracking, the bottom layer tries to be de-bonded from the RC beam (Figure 24). This creates a weak link

in the three-sided jacket; therefore, the jacket becomes ineffective at the post-peak stage that results in a flexure–shear failure with less deformation capacity.

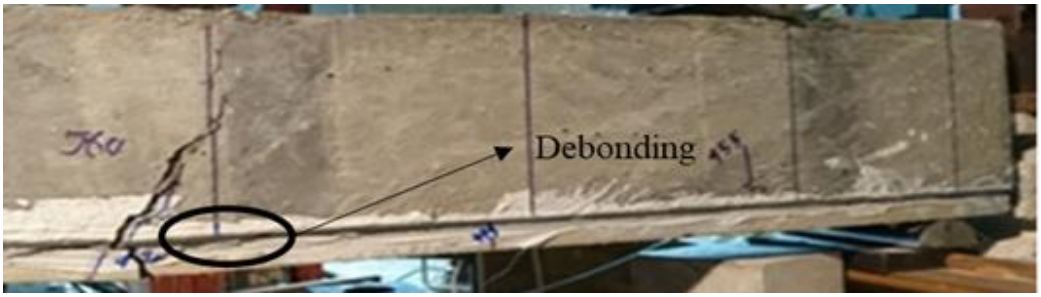

Figure 24. The problem of epoxy adhesive strengthening beam. Adapted from Ref. [74].

3.4. Effect of UHPC Compressive Strength

The improvement in maximum load capacity with UHPC compressive strength, using the experimental database, is plotted in Figure 25. It is evident that the improvement in ultimate load capacity enhances with the increase in UHPC compressive strength irrespective of the strengthening configuration. The enhancement in the ultimate capacity improvement can be attributed to the improved flexural capacity of the strengthened RC section with the increase in UHPC compressive strength.

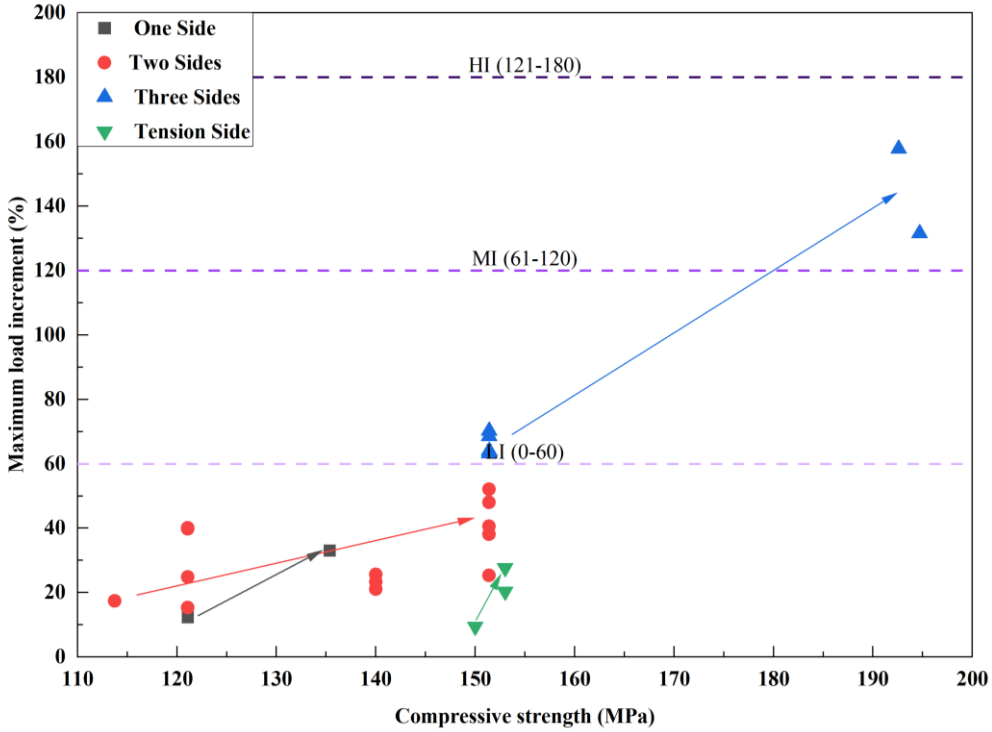

Figure 25. Effect of compressive strength on maximum load [73–75,81–83,89].

3.5. Effect of Steel Fiber Percentage

The improvements in maximum and cracking load capacity with steel fiber percentages, using the experimental database, are plotted in Figures 26 and 27, respectively. The analysis results demonstrate that the percentage of steel fiber has less impact on the ultimate and cracking load improvement, especially for the two-sided strengthening scheme.

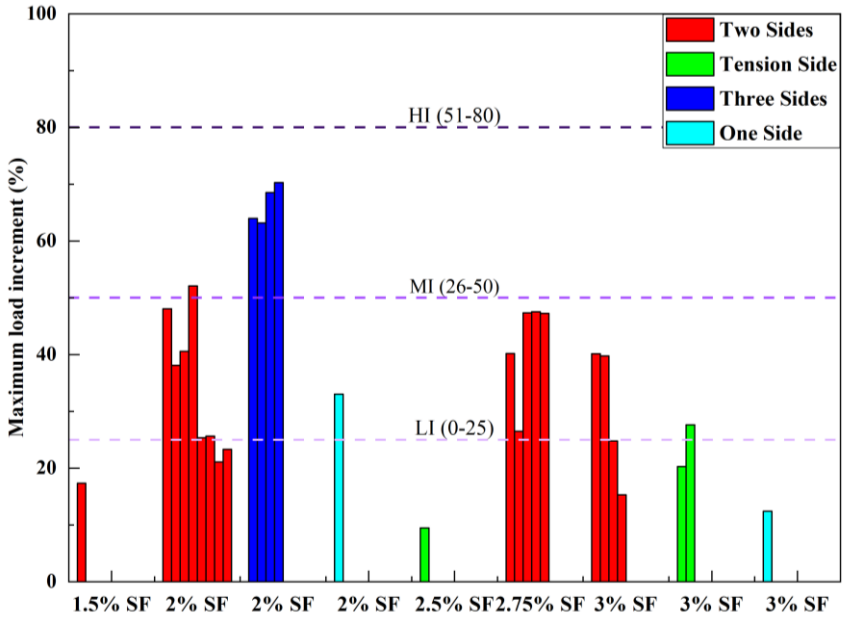

Figure 26. Effect of steel fiber percentage on maximum load increment [73–75,81–84,89].

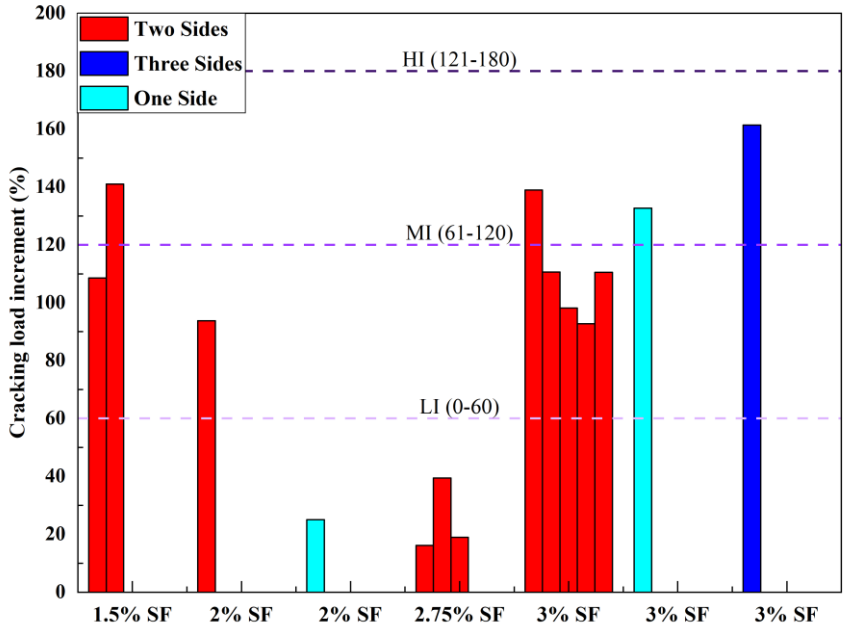

Figure 27. Effect of steel fiber percentage on cracking load [73–75,81–84,89].

4. Conclusions

This study presents a comprehensive evaluation of all experimental studies on the flexural and shear strengthening of RC beams with the UHPC layers. This study investigated the effects of (1) different retrofitting configurations, (2) the shear span and strengthening layer thickness ratio, and (3) bonding techniques on the structural performance of RC beams. The research findings will be helpful for future code provisions. The major findings of this state-of-the-art review can be summarized as follows:

- RC beams strengthened on three sides demonstrated a better performance in terms of the cracking moment and maximum moment (falls in the high increment range). Nevertheless, the percentage of the cracking moment increment was higher than the percentage of the maximum moment. This behavior can be attributed to the presence

of fiber, which resulted in delayed crack opening due to the bridging effect between fiber and concrete.

- For flexural strengthening, the composite structure exhibited mostly monolithic behavior under mechanical loading, exhibiting a negligible slip at the interface and no debonding.
- Experimental studies on the shear strengthening of RC beams demonstrated that the three-side strengthening arrangement provided the best results in terms of load-carrying capacity (falls in the high increment range).
- As the shear span and strengthening layer thickness ratio increased, the percentage of the load increment decreased after a specific range.
- The shear span, strengthening configurations, and strengthening layer thickness ratios have a remarkable effect on altering the failure mode in the case of shear strengthening.
- Effective depth and strengthening layer thickness ratios have shown a nonlinear effect on the percentage of the moment increment (cracking and maximum) in different strengthening configurations.
- In summary, the investigation results revealed that the three-side strengthening exhibits a notably higher range of the increment for both flexural (maximum at 81–120% and cracking at 300–500%) and shear (maximum at 51–80% and cracking at 121–180%) strengthening when compared to other strengthening configurations, encompassing all other parameters.

In addition to the aforementioned conclusions, future studies should consider the following aspects:

- In the case of flexural strengthening, UHPC and concrete substrates sometimes behave separately due to (1) localized macro-cracks between the old concrete structure and UHPC layer; and (2) an improper distribution of steel fiber in UHPC casting. These factors need to be considered in future studies.
- Most of the studies in the literature focused on strengthening (flexural and shear) of the RC beams in uncracked conditions, which does not represent the actual behavior of the damaged structure. So, future studies should consider strengthening the damaged RC beams.
- Flexural and shear strengthening of corroded RC beams with different configurations of UHPC layers needs to be investigated.
- The past studies mainly focused on static loading, with a few explorations into cyclic loading. So, further investigation is required to understand the response to cyclic loading, including factors like fatigue and seismic loading.
- For cast-in situ applications, tensile stresses are generated due to the high shrinkage of UHPC, which creates a threat of a debonding/slip at the surface between concrete and UHPC layers. Thus, a proper guideline needs to be developed in cases of water jetting and concrete chipping.

Author Contributions: Conceptualization, R.K.B. and F.B.A.; methodology, F.B.A. and R.K.B.; software, F.B.A. and S.T.; validation, D.S. and R.K.B.; formal analysis, F.B.A.; investigation, F.B.A.; resources, F.B.A.; data curation, F.B.A. and S.T.; writing—original draft preparation, F.B.A.; writing—review and editing, R.K.B. and D.S.; visualization, F.B.A., S.T., and R.K.B.; supervision, R.K.B. All authors have read and agreed to the published version of the manuscript.

Funding: This research received no external funding.

Data Availability Statement: The data that support the findings of this study are available from the corresponding author upon reasonable request.

Conflicts of Interest: The authors have no conflicts of interest to declare that are relevant to the content of this article. Rajib Kumar Biswas has no conflicts from Okumura Corporation.

References

1. Alaee, F.J.; Karihaloo, B.L. Retrofitting of Reinforced Concrete Beams with CARDIFRC. *J. Compos. Constr.* **2003**, *7*, 174–186. [CrossRef]
2. Lee, M.G.; Wang, Y.C.; Chiu, C.T. A Preliminary Study of Reactive Powder Concrete as a New Repair Material. *Constr. Build. Mater.* **2007**, *21*, 182–189. [CrossRef]
3. Biswas, R.K.; Iwanami, M.; Chijiwa, N.; Uno, K. Effect of Non-Uniform Rebar Corrosion on Structural Performance of RC Structures: A Numerical and Experimental Investigation. *Constr. Build. Mater.* **2020**, *230*, 116908. [CrossRef]
4. Biswas, R.K.; Iwanami, M.; Chijiwa, N.; Uno, K. Finite Element Analysis of RC Beams Subjected to Non-Uniform Corrosion of Steel Bars. In Proceedings of the 5th International Conference on Sustainable Construction Materials and Technologies (SCMT5), London, UK, 15–17 July 2019.
5. Biswas, R.K.; Iwanami, M.; Chijiwa, N.; Nakayama, K. Numerical Evaluation on the Effect of Steel Bar Corrosion on the Cyclic Behaviour of RC Bridge Piers. *Mater. Today Proc.* **2021**, *44*, 2393–2398. [CrossRef]
6. Biswas, R.K.; Iwanami, M.; Chijiwa, N.; Nakayama, K. Structural Assessment of the Coupled Inf luence of Corrosion Damage and Seismic Force on the Cyclic Behaviour of RC Columns. *Constr. Build. Mater.* **2021**, *304*, 124706. [CrossRef]
7. Biswas, R.K.; Iwanami, M.; Chijiwa, N.; Saito, T.; Malaga-Chuquitaype, C. A Simplified Approach to Evaluate Cyclic Response and Seismic Fragility of Corrosion Damaged RC Bridge Piers. *Dev. Built Environ.* **2022**, *12*, 100083. [CrossRef]
8. Datta, D. Electrospun Recycled Polyethylene Terephthalate Microfibers as an Asphalt Mix Additive. Master's Thesis, South Dakota State University, Brookings, SD, USA, 2023.
9. Biswas, R.K.; Iwanami, M.; Chijiwa, N.; Saito, T. The Effect of Non-Uniform Steel Bar Corrosion on Pre-Stressed RC Members Subjected to Hysteretic Load at the Mid-Span: Experimental Study and Three-Dimensional FEM Modeling. *Arch. Civ. Mech. Eng.* **2023**, *23*, 163. [CrossRef]
10. El Kechebour, B.; Zeloum, H. Choice between Retrofitting and Reconstruction of Buildings in Reinforced Concrete after an Earthquake. *Adv. Mater. Res.* **2015**, *1119*, 736–740. [CrossRef]
11. Brühwiler, E. Rehabilitation of Concrete Bridges Using Ultra-High Fibre Reinforced Concrete (UHPFRC). In Proceedings of the 3rd International Symposium on Life-Cycle Civil Engineering, Vienna, Austria, 3–6 October 2012; Strauss, A., Frangopol, D.K., Eds.; CRC Press: Vienna, Austria, 2012; pp. 1934–1941.
12. Jose, J.; Nagarajan, P.; Remanan, M. Utilisation of Ultra-High Performance Fiber Reinforced Concrete(UHPFRC) for Retroffiting—A Review. In Proceedings of the International Conference on Materials, Mechanics and Structures 2020 (ICMMS2020); IOP Conf. Series: Materials Science and Engineering, Online, 14–15 July 2020; Volume 936, pp. 1–8.
13. Oehlers, D.J. Reinforced Concrete Beams with Plates Glued to Their Soffits. *J. Struct. Eng.* **1992**, *118*, 2023–2038. [CrossRef]
14. Souza, R.H.F.; Appleton, J. Flexural Behaviour of Strengthened Reinforced Concrete Beams. *Mater. Struct.* **1997**, *30*, 154–159. [CrossRef]
15. Yurdakul, Ö.; Avşar, Ö. Strengthening of Substandard Reinforced Concrete Beam-Column Joints by External Post-Tension Rods. *Eng. Struct.* **2016**, *107*, 9–22. [CrossRef]
16. Altun, F. An Experimental Study of the Jacketed Reinforced-Concrete Beams under Bending. *Constr. Build. Mater.* **2004**, *18*, 611–618. [CrossRef]
17. Alhadid, M.M.A.; Youssef, M.A. Analysis of Reinforced Concrete Beams Strengthened Using Concrete Jackets. *Eng. Struct.* **2017**, *132*, 172–187. [CrossRef]
18. Tetta, Z.C.; Koutas, L.N.; Bournas, D.A. Textile-Reinforced Mortar (TRM) versus Fiber-Reinforced Polymers (FRP) in Shear Strengthening of Concrete Beams. *Compos. Part B Eng.* **2015**, *77*, 338–348. [CrossRef]
19. Spadea, G.; Bencardino, F.; Swamy, R.N. Structural Behavior of Composite RC Beams with Externally Bonded CFRP. *J. Compos. Constr.* **1998**, *2*, 132–137. [CrossRef]
20. Lamanna, A.J.; Bank, L.C.; Scott, D.W. Flexural Strengthening of Reinforced Concrete Beams by Mechanically Attaching Fiber-Reinforced Polymer Strips. *J. Compos. Constr.* **2004**, *8*, 203–210. [CrossRef]
21. Al-Saidy, A.H.; Saadatmanesh, H.; El-Gamal, S.; Al-Jabri, K.S.; Waris, B.M. Structural Behavior of Corroded RC Beams with/without Stirrups Repaired with CFRP Sheets. *Mater. Struct.* **2015**, *49*, 3733–3747. [CrossRef]
22. Thermou, G.E.; Pantazopoulou, S.J.; Elnashai, A.S. Flexural Behavior of Brittle RC Members Rehabilitated with Concrete Jacketing. *J. Struct. Eng.* **2007**, *133*, 1373–1384. [CrossRef]
23. Holman, J.W.; Cook, J.P. Steel Plates for Torsion Repair of Concrete Beams. *J. Struct. Eng.* **1984**, *110*, 10–18. [CrossRef]
24. Wu, Z.J.; Davies, J.M. Mechanical Analysis of a Cracked Beam Reinforced with an External FRP Plate. *Compos. Struct.* **2003**, *62*, 139–143. [CrossRef]
25. Triantafillou, T.C.; Plevris, N. Strengthening of RC Beams with Epoxy-Bonded Fibre-Composite Materials. *Mater. Struct.* **1992**, *25*, 201–211. [CrossRef]
26. D'Ambrisi, A.; Focacci, F. Flexural Strengthening of RC Beams with Cement-Based Composites. *J. Compos. Constr.* **2011**, *15*, 707–720. [CrossRef]
27. de Sena Cruz, J.M.; Oliveira de Barros, J.A. Bond Between Near-Surface Mounted Carbon-Fiber-Reinforced Polymer Laminate Strips and Concrete. *J. Compos. Constr.* **2004**, *8*, 519–527. [CrossRef]
28. Harajli, M.H.; Soudki, K.A.; Kudsi, T. Strengthening of Interior Slab–Column Connections Using a Combination of FRP Sheets and Steel Bolts. *J. Compos. Constr.* **2006**, *10*, 399–409. [CrossRef]

29. Zhou, M.; Lu, W.; Song, J.; Lee, G.C. Application of Ultra-High Performance Concrete in Bridge Engineering. *Constr. Build. Mater.* **2018**, *186*, 1256–1267. [CrossRef]
30. Tanarslan, H.M.; Alver, N.İ.N.E.L.; Jahangiri, R.; Yalçınkaya, Ç.; Yazıcı, H. Flexural Strengthening of RC Beams Using UHPFRC Laminates: Bonding Techniques and Rebar Addition. *Constr. Build. Mater.* **2017**, *155*, 45–55. [CrossRef]
31. Sharma, R.; Bansal, P.P. Behavior of RC Exterior Beam Column Joint Retrofitted Using UHP-HFRC. *Constr. Build. Mater.* **2019**, *195*, 376–389. [CrossRef]
32. Prem, P.R.; Murthy, A.R. Acoustic Emission and Flexural Behaviour of RC Beams Strengthened with UHPC Overlay. *Constr. Build. Mater.* **2016**, *123*, 481–492. [CrossRef]
33. Al-Osta, M.A.; Isa, M.N.; Baluch, M.H.; Rahman, M.K. Flexural Behavior of Reinforced Concrete Beams Strengthened with Ultra-High Performance Fiber Reinforced Concrete. *Constr. Build. Mater.* **2017**, *134*, 279–296. [CrossRef]
34. Mohammed, T.J.B.B.H.; Bunnori, N.M. Strengthening of Reinforced Concrete Beams Subjected to Torsion with UHPFC Composites. *Struct. Eng. Mech.* **2015**, *56*, 123–136. [CrossRef]
35. Abdullah, M.A.H.; Mohd Zahid, M.Z.A.; Abu Bakar, B.H.; Nazri, F.M.; Ayob, A. UHPFRC as Repair Material for Fire-Damaged Reinforced Concrete Structure—A Review. *Appl. Mech. Mater.* **2015**, *802*, 283–289. [CrossRef]
36. Garg, V.; Bansal, P.P.; Sharma, R. Retrofitting of Shear-Deficient RC Beams Using UHP-FRC. *Iran. J. Sci. Technol. Trans. Civ. Eng.* **2019**, *43*, 419–428. [CrossRef]
37. Paschalis, S.A.; Lampropoulos, A.P.; Tsioulou, O. Experimental and Numerical Study of the Performance of Ultra High Performance Fiber Reinforced Concrete for the Flexural Strengthening of Full Scale Reinforced Concrete Members. *Constr. Build. Mater.* **2018**, *186*, 351–366. [CrossRef]
38. Mansour, W.; Tayeh, B.A. Shear Behaviour of RC Beams Strengthened by Various Ultrahigh Performance Fibre-Reinforced Concrete Systems. *Adv. Civ. Eng.* **2020**, *2020*, 2139054. [CrossRef]
39. Ramachandra Murthy, A.; Karihaloo, B.L.; Priya, D.S. Flexural Behavior of RC Beams Retrofitted with Ultra-High Strength Concrete. *Constr. Build. Mater.* **2018**, *175*, 815–824. [CrossRef]
40. Habel, K.; Denarié, E.; Brühwiler, E. Experimental Investigation of Composite-High-Performance Fiber-Reinforced and Conventional Concrete Members. *Struct. J.* **2007**, *104*, 93–101. [CrossRef]
41. Prem, P.R.; Murthy, A.R.; Verma, M. Theoretical Modelling and Acoustic Emission Monitoring of RC Beams Strengthened with UHPC. *Constr. Build. Mater.* **2018**, *158*, 670–682. [CrossRef]
42. Biswas, R.K.; Saito, T.; Misawa, T.; Iwanami, M. Structural Behavior of Severely Corroded RC Beams Retrofitted with UHPC Layer: An Experimental Study. *Innov. Infrastruct. Solut.* **2023**, *8*, 322. [CrossRef]
43. Graybeal, B.A. *Material Property Characterization of Ultra-High Performance Concrete*; Turner Fairbank Highway Research Center: McLean, VA, USA, 2006.
44. Rahman, S.; Molyneaux, T.; Patnaikuni, I. Ultra High Performance Concrete: Recent Applications and Research. *Aust. J. Civ. Eng.* **2015**, *2*, 13–20. [CrossRef]
45. Graybeal, B.A.; Baby, F. Development of Direct Tension Test Method for Ultra-High-Performance Fiber-Reinforced Concrete. *ACI Mater. J.* **2013**, *110*, 177–186.
46. Ahlborn, T.M.; Harris, D.K.; Misson, D.L.; Peuse, E.J. Strength and Durability Characterization of Ultra-High Performance Concrete Under Variable Curing Conditions—MOB Lab. In Proceedings of the Transportation Research Board (TRB) 90th Annual Meeting, Washington, DC, USA, 23–27 January 2011; pp. 68–75.
47. Tai, Y.S.; Pan, H.H.; Kung, Y.N. Mechanical Properties of Steel Fiber Reinforced Reactive Powder Concrete Following Exposure to High Temperature Reaching 800 °C. *Nucl. Eng. Des.* **2011**, *241*, 2416–2424. [CrossRef]
48. Voo, Y.L.; Foster, S.J.; Voo, C.C. Ultrahigh-Performance Concrete Segmental Bridge Technology: Toward Sustainable Bridge Construction. *J. Bridge Eng.* **2015**, *20*, B5014001. [CrossRef]
49. Yu, R.; Song, Q.; Wang, X.; Zhang, Z.; Shui, Z.; Brouwers, H.J.H. Sustainable Development of Ultra-High Performance Fibre Reinforced Concrete (UHPFRC): Towards to an Optimized Concrete Matrix and Efficient Fibre Application. *J. Clean. Prod.* **2017**, *162*, 220–233. [CrossRef]
50. Ghabchi, R.; Datta, D.; Mihandoust, M. Utilization of Recycled Electronics Waste (E-Waste) in Portland Cement Concrete. In Proceedings of the International Conference on Transportation and Development 2022: Application of Emerging Technologies—Selected Papers from the Proceedings of the International Conference on Transportation and Development, Seattle, DC, USA, 31 May–3 June 2022; Wei, H., Ed.; American Society of Civil Engineers: Seattle, DC, USA, 2022; Volume 5, pp. 318–326.
51. Shi, C.; Wu, Z.; Xiao, J.; Wang, D.; Huang, Z.; Fang, Z. A Review on Ultra High Performance Concrete: Part I. Raw Materials and Mixture Design. *Constr. Build. Mater.* **2015**, *101*, 741–751. [CrossRef]
52. Martin-Sanz, H.; Chatzi, E.; Brühwiler, E. The Use of Ultra High Performance Fibre Reinforced Cement-Based Composites in Rehabilitation Projects: A Review. In Proceedings of the 9th International Conference on Fracture Mechanics of Concrete and Concrete Structures, Berkeley, CA, USA, 29 May–1 June 2016; pp. 1–12.
53. Tahwia, A.M.; Elgendy, G.M.; Amin, M. Durability and Microstructure of Eco-Efficient Ultra-High-Performance Concrete. *Constr. Build. Mater.* **2021**, *303*, 124491. [CrossRef]
54. Sohail, M.G.; Kahraman, R.; al Nuaimi, N.; Gencturk, B.; Alnahhal, W. Durability Characteristics of High and Ultra-High Performance Concretes. *J. Build. Eng.* **2021**, *33*, 101669. [CrossRef]

55. Matos, A.M.; Chaves Figueiredo, S.; Nunes, S.; Schlangen, E.; Barroso-Aguiar, J.L. Durability of an UHPFRC under Mechanical and Chloride Loads. *Constr. Build. Mater.* **2021**, *311*, 125223. [CrossRef]
56. Wang, D.; Shi, C.; Wu, Z.; Xiao, J.; Huang, Z.; Fang, Z. A Review on Ultra High Performance Concrete: Part II. Hydration, Microstructure and Properties. *Constr. Build. Mater.* **2015**, *96*, 368–377. [CrossRef]
57. Brühwiler, E.; Denarié, E. Rehabilitation of Concrete Structures Using Ultra-High Performance Fibre Reinforced Concrete. In Proceedings of the UHPC-2008: The Second International Symposium on Ultra High Performance Concrete, Kassel, Germany, 5–7 March 2008; pp. 1–8.
58. Denarié, E.; Brühwiler, E. Structural Rehabilitations with Ultra High Performance Fibre Reinforced Concretes. *Int. J. Restor. Build. Monum.* **2006**, *12*, 453–465.
59. Rossi, P. Development of New Cement Composite Materials for Construction. *Proc. Inst. Mech. Eng. Part L J. Mater. Des. Appl.* **2005**, *219*, 67–74. [CrossRef]
60. Abdal, S.; Mansour, W.; Agwa, I.; Nasr, M.; Abadel, A.; Onuralp Özkılıç, Y.; Akeed, M.H. Application of Ultra-High-Performance Concrete in Bridge Engineering: Current Status, Limitations, Challenges, and Future Prospects. *Buildings* **2023**, *13*, 185. [CrossRef]
61. Habel, K.; Viviani, M.; Denarié, E.; Brühwiler, E. Development of the Mechanical Properties of an Ultra-High Performance Fiber Reinforced Concrete (UHPFRC). *Cem. Concr. Res.* **2006**, *36*, 1362–1370. [CrossRef]
62. Xue, J.; Briseghella, B.; Huang, F.; Nuti, C.; Tabatabai, H.; Chen, B. Review of Ultra-High Performance Concrete and Its Application in Bridge Engineering. *Constr. Build. Mater.* **2020**, *260*, 119844. [CrossRef]
63. Brühwiler, E. "Structural UHPFRC": Welcome to the Post-Concrete Era! In Proceedings of the International Interactive Symposium on Ultra-High Performance Concrete, Des Moines, IA, USA, 18–20 July 2016; Iowa State University Digital Press: Ames, IA, USA, 2016; Volume 1.
64. Wille, K.; Naaman, A.E.; Parra-Montesinos, G.J. Ultra-High Performance Concrete with Compressive Strength Exceeding 150 MPa (22 Ksi): A Simpler Way. *ACI Mater. J.* **2011**, *108*, 46–54. [CrossRef]
65. Yoo, D.Y.; Kang, S.T.; Yoon, Y.S. Effect of Fiber Length and Placement Method on Flexural Behavior, Tension-Softening Curve, and Fiber Distribution Characteristics of UHPFRC. *Constr. Build. Mater.* **2014**, *64*, 67–81. [CrossRef]
66. Wille, K.; Kim, D.J.; Naaman, A.E. Strain-Hardening UHP-FRC with Low Fiber Contents. *Mater. Struct.* **2011**, *44*, 583–598. [CrossRef]
67. Yoo, D.Y.; Banthia, N. Mechanical Properties of Ultra-High-Performance Fiber-Reinforced Concrete: A Review. *Cem. Concr. Compos.* **2016**, *73*, 267–280. [CrossRef]
68. Biswas, R.K.; bin Ahmed, F.; Haque, M.E.; Provasha, A.A.; Hasan, Z.; Hayat, F.; Sen, D. Effects of Steel Fiber Percentage and Aspect Ratios on Fresh and Harden Properties of Ultra-High Performance Fiber Reinforced Concrete. *Appl. Mech.* **2021**, *2*, 501–515. [CrossRef]
69. Huang, Y.; Grünewald, S.; Schlangen, E.; Luković, M. Strengthening of Concrete Structures with Ultra High Performance Fiber Reinforced Concrete (UHPFRC): A Critical Review. *Constr. Build. Mater.* **2022**, *336*, 127398. [CrossRef]
70. Resplendino, J. Ultra High Performance Concrete: New AFGC Recommendations. In *Designing and Building with UHPFRC.*; Wiley: Hoboken, NJ, USA, 2013; pp. 713–722. [CrossRef]
71. Yokota, H.; Rokugo, K.; Sakata, N. *JSCE Recommendations for Design and Construction of High Performance Fiber Reinforced Cement Composite with Multiple Fine Cracks*; Japan Society of Civil Engineers: Tokyo, Japan, 2008.
72. Paschalis, S.A. Strengthening of Existing Reinforced Concrete Structures Using Ultra High Performance Fiber Reinforced Concrete. Doctoral Thesis, University of Brighton, Brighton, UK, 2017.
73. Bahraq, A.A.; Al-Osta, M.A.; Ahmad, S.; Al-Zahrani, M.M.; Al-Dulaijan, S.O.; Rahman, M.K. Experimental and Numerical Investigation of Shear Behavior of RC Beams Strengthened by Ultra-High Performance Concrete. *Int. J. Concr. Struct. Mater.* **2019**, *13*, 6. [CrossRef]
74. Bahraq, A.A.A. Shear Behaviour of RC Beams Strengthened by Ultra- High Performance Concrete (UHPC). Master's Thesis, King Fahd University of Petroleum and Minerals, Dhahran, Saudi Arabia, 2017.
75. Yin, H.; Teo, W.; Shirai, K. Experimental Investigation on the Behaviour of Reinforced Concrete Slabs Strengthened with Ultra-High Performance Concrete. *Constr. Build. Mater.* **2017**, *155*, 463–474. [CrossRef]
76. Safdar, M.; Matsumoto, T.; Kakuma, K. Flexural Behavior of Reinforced Concrete Beams Repaired with Ultra-High Performance Fiber Reinforced Concrete (UHPFRC). *Compos. Struct.* **2016**, *157*, 448–460. [CrossRef]
77. Anusree, K.; Anuragi, P. Study on Strengthening of RC Beams Overlaying With UHPFRC. *Int. J. Appl. Eng. Res.* **2019**, *14*, 12–16.
78. Tanarslan, H.M. Flexural Strengthening of RC Beams with Prefabricated Ultra High Performance Fibre Reinforced Concrete Laminates. *Eng. Struct.* **2017**, *151*, 337–348. [CrossRef]
79. Zhu, Y.; Zhang, Y.; Hussein, H.H.; Chen, G. Flexural Strengthening of Reinforced Concrete Beams or Slabs Using Ultra-High Performance Concrete (UHPC): A State of the Art Review. *Eng. Struct.* **2020**, *205*, 110035. [CrossRef]
80. Meda, A.; Plizzari, G.A.; Rinaldi, Z.; Martinola, G. Strengthening of R/C Existing Columns with High Performance Fiber Reinforced Concrete Jacket. In Proceedings of the Concrete Repair, Rehabilitation and Retrofitting II: 2nd International Conference on Concrete Repair, Rehabilitation and Retrofitting, Cape Town, South Africa, 24–26 November 2008; Alexander, M.G., Beushausen, H.-D., Dehn, F., Moyo, P., Eds.; CRC Press: Stellenbosch, South Africa, 2008; pp. 443–445.

81. Sakr, M.A.; Sleemah, A.A.; Khalifa, T.M.; Mansour, W.N. Shear Strengthening of Reinforced Concrete Beams Using Prefabricated Ultra-High Performance Fiber Reinforced Concrete Plates: Experimental and Numerical Investigation. *Struct. Concr.* **2019**, *20*, 1137–1153. [CrossRef]
82. Sakr, M.A.; Sleemah, A.A.; Khalifa, T.M.; Mansour, W.N. Behavior of RC Beams Strengthened in Shear with Ultra-High Performance Fiber Reinforced Concrete (UHPFRC). In Proceedings of the International Conference on Concrete Repair, Rehabilitation and Retrofitting; MATEC Web Conference, Cape Town, South Africa, 19–21 November 2018; Volume 199, pp. 1–5.
83. Aghani, K.; Afshin, H. Experimental and Numerical Investigation on Shear Retrofitting of RC Beams by Prefabricated UHPFRC Sheets. *Civ. Eng. J.* **2016**, *2*, 168–179. [CrossRef]
84. Tanarslan, H.M.; Yalçınkaya, Ç.; Alver, N.; Karademir, C. Shear Strengthening of RC Beams with Externally Bonded UHPFRC Laminates. *Compos. Struct.* **2021**, *262*, 113611. [CrossRef]
85. He, J.; Chao, L. Numerical Analysis on Shear Resistance of Ultra-High Performance Concrete-Normal Strength Concrete Composite Beam. *Struct. Concr.* **2021**, *22*, 1128–1146. [CrossRef]
86. Ji, H.; Liu, C. Ultimate Shear Resistance of Ultra-High Performance Fiber Reinforced Concrete-Normal Strength Concrete Beam. *Eng. Struct.* **2020**, *203*, 109825. [CrossRef]
87. Wirojjanapirom, P.; Matsumoto, K.; Kono, K.; Niwa, J. Experimental Study on Shear Behavior of RC Beams Using U-Shaped UFC Permanent Formwork with Shear Keys and Bolts. *J. Jpn. Soc. Civ. Eng. Ser. E2 (Mater. Concr. Struct.)* **2013**, *69*, 67–81. [CrossRef]
88. Wirojjanapirom, P.; Matsumoto, K.; Kono, K.; Niwa, J. Shear Behavior of RC Beams Using U-Shaped UFC Permanent Formwork with Shear Keys or Bolts. *Concr. Res. Technol.* **2011**, *33*, 1537–1542. [CrossRef]
89. Said, A.; Elsayed, M.; El-Azim, A.A.; Althoey, F.; Tayeh, B.A. Using Ultra-High Performance Fiber Reinforced Concrete in Improvement Shear Strength of Reinforced Concrete Beams. *Case Stud. Constr. Mater.* **2022**, *16*, e01009. [CrossRef]
90. Nadir, W.; Kadhimi, M.M.A.; Jawdhari, A.; Fam, A.; Majdi, A. RC Beams Strengthened in Shear with FRP-Reinforced UHPC Overlay: An Experimental and Numerical Study. *Structures* **2023**, *53*, 693–715. [CrossRef]